the plant journal

SEB SOCIETY FOR EXPERIMENTAL BIOLOGY

The Plant Journal (2025) **121,** e17179 doi: 10.1111/tpj.17179

The calcium sensor AtCML8 contributes to Arabidopsis plant cell growth by modulating the brassinosteroid signaling pathway

Amandine Lucchin, Hélène Fouassier, Eugénie Robe, Malick Mbengue, Marielle Aguilar, Hélène San Clemente, Grégory Vert, Jean-Philippe Galaud and Didier Aldon*

Laboratoire de Recherche en Sciences Végétales, Université de Toulouse, CNRS, UPS, Toulouse INP, 24, chemin de Borde Rouge, Auzeville-Tolosane 31320, France

Received 13 April 2024; revised 26 September 2024; accepted 14 November 2024; published online 2 December 2024.
*For correspondence (e-mail didier.aldon@univ-tlse3.fr).

SUMMARY

Calcium signaling plays an essential role in integrating plant responses to diverse stimuli and regulating growth and development. While some signaling components and their roles are well-established, such as the ubiquitous calmodulin (CaM) sensor, plants possess a broader repertoire of calcium sensors. Notably, CaM-like proteins (CMLs) represent a poorly characterized class for which interacting partners and biological functions remain largely elusive. Our work investigates the role of *Arabidopsis thaliana* CML8 that exhibits a unique expression profile in seedlings. A reverse genetic approach revealed a function of CML8 in regulating root growth and hypocotyl elongation. RNA-seq analyses highlighted CML8 association with the regulation of numerous genes involved in growth and brassinosteroid (BR) signaling. Using co-immunoprecipitation experiments, we demonstrated that CML8 interacts with the BR receptor, BRI1, *in planta* in a ligand-dependent manner. This finding suggests the existence of a novel regulatory step in the BR pathway, involving calcium signaling.

Keywords: calcium signaling, calmodulin-like, brassinosteroid, root growth, hypocotyl, *Arabidopsis thaliana*.

INTRODUCTION

Terrestrial plants have the capacity to grow in and adapt to diverse environments, and this is mainly due to their great phenotypic plasticity. Plants have evolved systems to perceive and signal fluctuations in their biotic or abiotic environment, ensuring the execution of responses adapted in nature and intensity to the perceived stimuli. Plant hormones are central components of these responses and contribute to modulating growth and developmental transitions at the plant level or organ scale (Benkova, 2016; Chaiwanon et al., 2016; Vanstraelen & Benkova, 2012). Calcium signaling can act upstream or downstream of hormonal pathways to integrate external stimuli at the cellular level allowing the initiation of adapted physiological and developmental responses (Hepler, 2005; Tian et al., 2020). Transient variations in the concentration of free intracellular calcium ($[Ca^{2+}]_{int}$) can be recorded when plants are exposed to stresses but also during plant cell growth and development (Hepler, 2005; Leitao et al., 2019; Luan & Wang, 2021). These $[Ca^{2+}]_{int}$ variations are often referred to as calcium signatures, as they reflect on the nature and intensity of the initial stimulus at the cellular level (McAinsh & Pittman, 2009). The $[Ca^{2+}]_{int}$ increase is sensed by a set of calcium sensor proteins, the best characterized being calmodulins (CaMs) (Perochon et al., 2011; Snedden & Fromm, 2001). This small protein is found in all eukaryotic cells and has no known intrinsic activity. CaMs can regulate the function of partner proteins known as CaM-binding proteins (CaM-BPs) (Bouche et al., 2005). CaM-BPs are diverse in nature, localization, or function, and after binding to CaMs, they can modify their sub-cellular localization, biochemical activities, or binding affinities to protein complexes (Bouche et al., 2005). The critical role of Ca^{2+}/calmodulin-mediated signaling in controlling the function of DWARF1 (DWF1), an enzyme that contributes to the brassinosteroid (BR) biosynthesis and therefore in the control of plant development, illustrates well the importance of such regulations (Du & Poovaiah, 2005). Genetic and molecular approaches revealed that loss of calmodulin binding completely abolished the function of DWF1 *in planta* (Du & Poovaiah, 2005). Many transcription factors have been identified as CaM-BPs. This

includes CaM-binding transcription activators (CAMTAs), CBP60s, WRKYs, MYBs, among others, which are implicated in various regulatory functions associated with development or responses to environmental stresses (Iqbal et al., 2020). In the model plant *Arabidopsis thaliana*, calmodulin is a highly conserved protein with four different isoforms encoded by seven genes. Each isoform differs from others by only 1–4 amino acids (McCormack et al., 2005). Due to functional redundancy, functional approaches on these proteins are difficult to undertake. In yeast, where only one gene encodes CaM (*CMD1*), deletion of *CMD1* results in a lethal mutation showing that yeast CaM is essential for cell function (Davis et al., 1986).

In plants, interest has been growing over the last two decades in proteins related to CaM, namely, the calmodulin-like proteins (CMLs) (McCormack et al., 2005; Zhu et al., 2015). The annotation of genes encoding CMLs and phylogenomic analyses suggest that CMLs may contribute to the adaptation of plants to their environment and to the control of developmental processes specific to a terrestrial lifestyle (Edel et al., 2017; Zhu et al., 2015). These hypotheses are supported by transcriptomic analyses that show specific expression profiles for *CMLs* at spatiotemporal level during plant development and in response to diverse stimuli (McCormack et al., 2005). Compared to canonical CaMs, this finding has opened the way to reverse genetics strategies to assess the contribution of CMLs in plant physiology. Several studies highlighted the contribution of CMLs to the establishment of defense processes or adaptation to abiotic stresses (Aldon et al., 2018; Ranty et al., 2016). For example, CML37 and CML42 in *A. thaliana* contribute positively and negatively to the resistance against the herbivorous insect *Spodoptera littoralis*, respectively (Scholz et al., 2014; Vadassery et al., 2012). Functional analyses have revealed a dual role for CML9, acting either as a negative regulator of drought stress (Magnan et al., 2008) or as a positive regulator of the plant immunity response to *Pseudomonas* strains (Leba et al., 2012). In Medicago, gain- or loss-of-function of *MtCML42* has been associated with cold tolerance and regulation of flowering time (Sun et al., 2021). In a developmental context, Arabidopsis *cml39* mutant seedlings exhibit an *in vitro* growth defect under carbon deficiency (Bender et al., 2013), prompting the authors to speculate on a role for this CML in light signaling during seedling growth (Bender et al., 2013). CML38 was described as a negative regulator of Arabidopsis root growth (Song et al., 2021). CML13 and CML14 have recently emerged as regulators with dual function, contributing to both developmental control (Symonds, Teresinski, Hau, Chiasson, et al., 2024) and stress responses such as salinity tolerance (Symonds, Teresinski, Hau, Dwivedi, et al., 2024).

Here, we report on the importance of CML8 in the control of seedling growth and development in *A. thaliana*. Previous works have highlighted the role of CML8 in the context of plant–microbe interactions and regulation of plant immunity (Zhu et al., 2017; Zhu et al., 2021). However, the specific expression patterns of *CML8* in growing organs or in lateral root primordia prompted us to evaluate its contribution to plant development. Here, we show that CML8 acts as a negative regulator of plant growth. We link CML8 function to the modulation of the BR signaling pathway in Arabidopsis through two mechanisms: (i) the *in planta* interaction of CML8 with the BR receptor BRI1 (*brassinosteroid insensitive 1*) (He et al., 2000) in a ligand-dependent manner and (ii) the modulation of the BR signaling pathway, resulting in significant gene reprograming and phenotypic outputs related to BRs.

RESULTS

CML8 expression is tightly regulated during plant development

To date, studies on CML8 have described its contribution during plant–microorganism interactions and have reported the inducible profile of *CML8* in response to phytopathogenic bacteria (Zhu et al., 2017, Zhu et al., 2021). Here, we describe the specific expression profile of *CML8*, during the early stages of seedling development and in particular tissues and organs (Figure 1). Under standard *in vitro* culture conditions, quantitative real-time PCR (RT-qPCR) analyses indicate that *CML8* is mainly expressed in the root system of young seedlings (Figure 1a). These data are consistent with publicly available transcriptome analyses (Zhang et al., 2020), showing that *CML8* is mainly expressed in the early stage of *A. thaliana* development in roots (Figure S1). We also used the web-based software tool Genevestigator (Hruz et al., 2008) to exploit available single-cell RNA analyses datasets and explore the expression profile of CML8 more broadly. These data indicate that *CML8* is more specifically expressed in the elongation zone of the primary root (PR), as well as in the rhizodermis, endodermis, lateral root cap, and columella cells (Figure S1). Altogether, this reveals a specific expression pattern for *CML8* in the early stages of seedling development (Figure 1).

In addition, previous works have shown that *CML8* expression can be induced in response to BRs, one of the major developmental hormones in plants (Chaiwanon & Wang, 2015; Clark et al., 2021). We then explore more closely the transcriptional regulation of *CML8* by BRs. The expression of *CML8* in response to epibrassinolide (eBL) treatment was assessed by RT-qPCR in young Arabidopsis seedlings. As shown Figure 1B, eBL application significantly induces the expression of *CML8* at early time points. Its expression is transiently increased 2-fold after 1 and 3 h of eBL application and returns to basal level after 6 h (Figure 1b). To obtain spatial information on

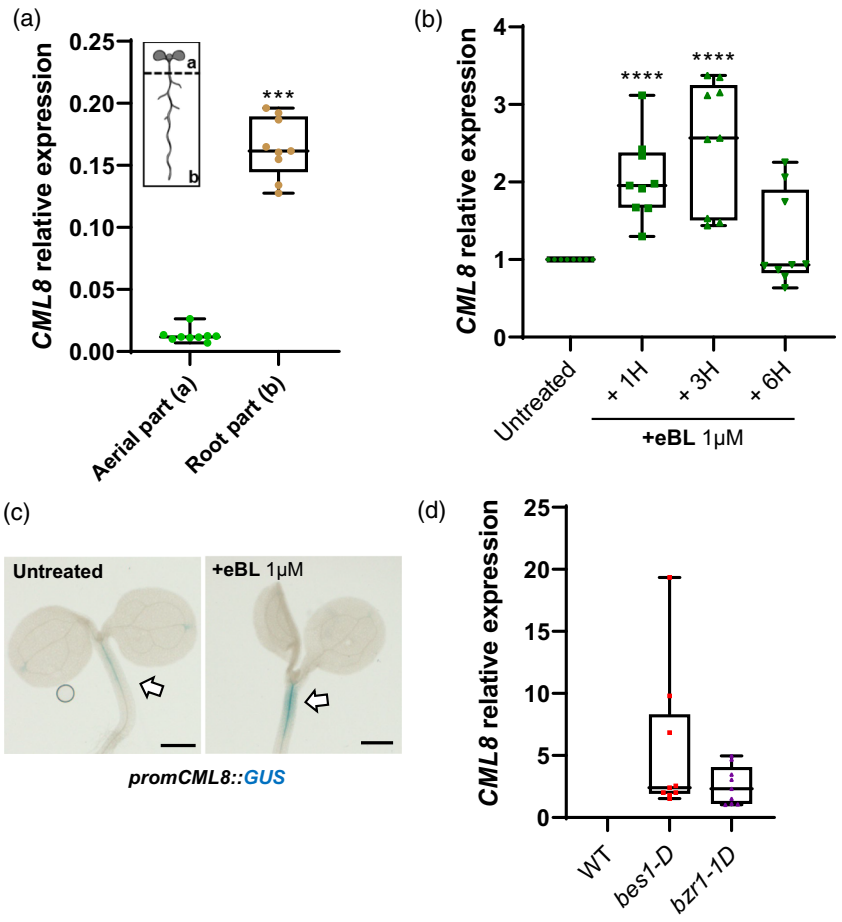

Figure 1. Expression profile of the *CML8* gene in *A. thaliana* seedlings grown under standard conditions or in response to exogenous application of brassinosteroids.
(a) *CML8* is predominantly expressed in the roots. RNA extraction was performed on separated aerial and root parts of untreated 7-d-old WT seedlings (Col8, Columbia-8).
(b) Kinetics of *CML8* expression by RT-qPCR show that this gene is quickly and transiently induced by exogenous application of epibrassinolides (eBL 1 μM). 7-day-old seedlings were treated or not with eBL (1 μM) for 1, 3, or 6 h.
(c) *CML8* promoter activity in response or not to eBL treatment is induced predominantly in hypocotyl (arrows). 7-d-old seedlings expressing the promCML8::*uidA* construct were treated or not for 3H with 1 μM eBL. Images are representative of at least three biological replicates. Scale bar = 0.05 mm.
(d) Quantitative analyses of *CML8* gene expression show significant inductions in *bes1-D* and *bzr1-1D* mutant lines. In (a), (b), and (c), the relative expression of *CML8* was determined by RT-qPCR, and the results shown are from the analysis of biological triplicates. Error bar = standard error of the mean. Statistical analysis was performed using a Wilcoxon–Mann–Whitney test (*P* value "****"<0.0001, "***"<0.001) (*n* = 9 for each experiment except in (c), where *n* = 8 for the untreated condition).

CML8 expression in response to BRs, we exposed a *promCML8-GUS* transcriptional reporter line to an exogenous eBL treatment for 3 h. GUS assays revealed a significant increase in the activity in the hypocotyl of 7-day-old seedlings (Figure 1c), pointing to a transcriptional control of *CML8* expression by eBL. To confirm the link between the transcriptional regulation of *CML8* and BR signaling, we quantified the expression of *CML8* in two gain-of-function mutants, *bes1-D* and *bzr1-1D* (Figure 1d). These two lines harbor a constitutive activity of the key transcriptional regulators BES1 (*bri1*-EMS suppressor 1) and BZR1 (brassinazole resistant 1), which acts downstream of BR perception by the BRI1 receptor (Kim & Wang, 2010). *CML8* gene is expressed three to five times more in these genetic backgrounds than in the wild type (WT) (Figure 1d), clearly connecting the BR signaling pathway to *CML8* regulation. Our analyses of publicly available transcriptome data using tools such as ACT (Zogopoulos et al., 2021), ATTED-II (Obayashi et al., 2022), and ARS (Yu et al., 2022) identified approximately 140 genes co-expressed with *CML8*. The genes co-expressed with *CML8* are enriched for functions associated with growth and development, particularly in root tissues. Given that *CML8* itself is an early BR-responsive gene, these findings suggest a potential role

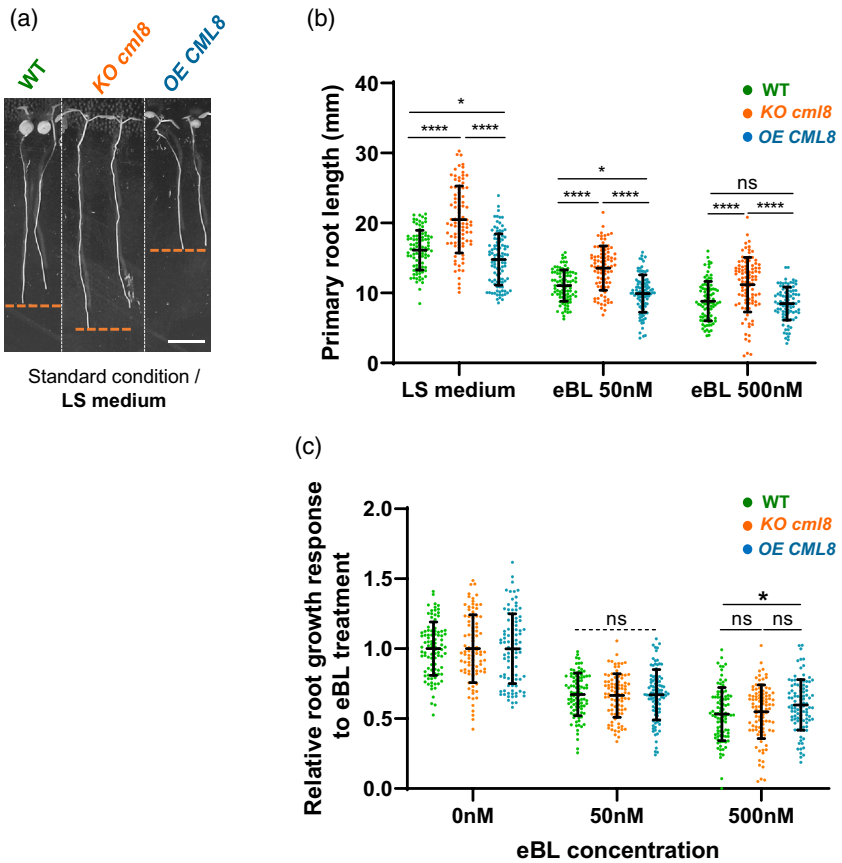

Figure 2. Analysis of root behavior of *Arabidopsis thaliana* WT and *cml8* mutant lines under standard and epibrassinolides (eBLs) treated conditions.
(a) Picture of a significant sample of 10-day-old seedlings (WT, Col8; KO *cml8* & OE *CML8*) pictured 5 days after they have been transferred to standard ½ LS agar culture medium. During the time of the root growth analysis experiment, the aerial parts have access to light, while the root system is kept in the dark. Scale bar = 1 cm.
(b) Quantitative analysis of PR length of the different genotypes after transfer under standard culture conditions (LS medium) or in response to the addition of increasing concentrations of eBL to the medium (50 and 500 nM).
(c) Normalized effect of exogenous epibrassinolide (eBL) application on root growth for each genotype relative to the standard condition (0 nM eBL). The data shown in (b) and (c) are from biological triplicates which represent a total of 87–97 values per genotype and tested condition. All individual data points are plotted. Black horizontal bars represent the means, and error bars represent the standard deviation. Statistical significance: Asterisks indicate significant differences between WT and *cml8* genotypes following two-way ANOVA with Tukey's multiple comparison test (*P* values that are represented as followed: "****"<0.0001; "**"<0.01; "*"<0.05; and "ns": not significant).

for CML8 in regulating BR-mediated growth processes, particularly at the seedling stage where it is most highly expressed.

CML8 acts as a negative regulator of seedling growth and modulates BR responses in *A. thaliana*

To gain insight into the physiological relevance of CML8 in developmental processes, we analyzed the phenotypes of seedlings grown under controlled *in vitro* conditions. Considering the expression profile of *CML8*, we were interested in root and hypocotyl growth. To determine whether CML8 plays a role in root growth, we quantified the PR growth of 10-day-old seedlings in gain- and loss-of-function lines ("*OE CML8*" and "KO *cml8*," respectively) compared to the reference WT line (Figure 2a). To ensure a correct genetic linkage between the phenotypes observed and the genotypes tested, all analyses were performed on two independent transgenic lines that overexpressed the *cml8* gene (OE *CML8* and OE *CML8 3.2* [Figures S3 and S4]) and a complemented *cml8* knockout (KO) transgenic line (named *cml8.2_C#13* in all the additional data and described in Figure S2c). Overexpressing lines have been previously characterized, and the *CML8* expression level is constitutively increased by 500- to 1000-fold in OE *CML8 3.2* and OE *CML8*, respectively, compared to the WT (Zhu et al., 2017). Complemented *cml8* KO transgenic lines were generated by reintroducing the *CML8* genomic sequence under the control of its native promoter region (Figure S2c), and the transgenic line that restored *CML8* expression closest to that of the WT was selected for all the phenotypic analyses (line *cml8.2_C#13* in Figure S2c; Figures S3c,d and S5).

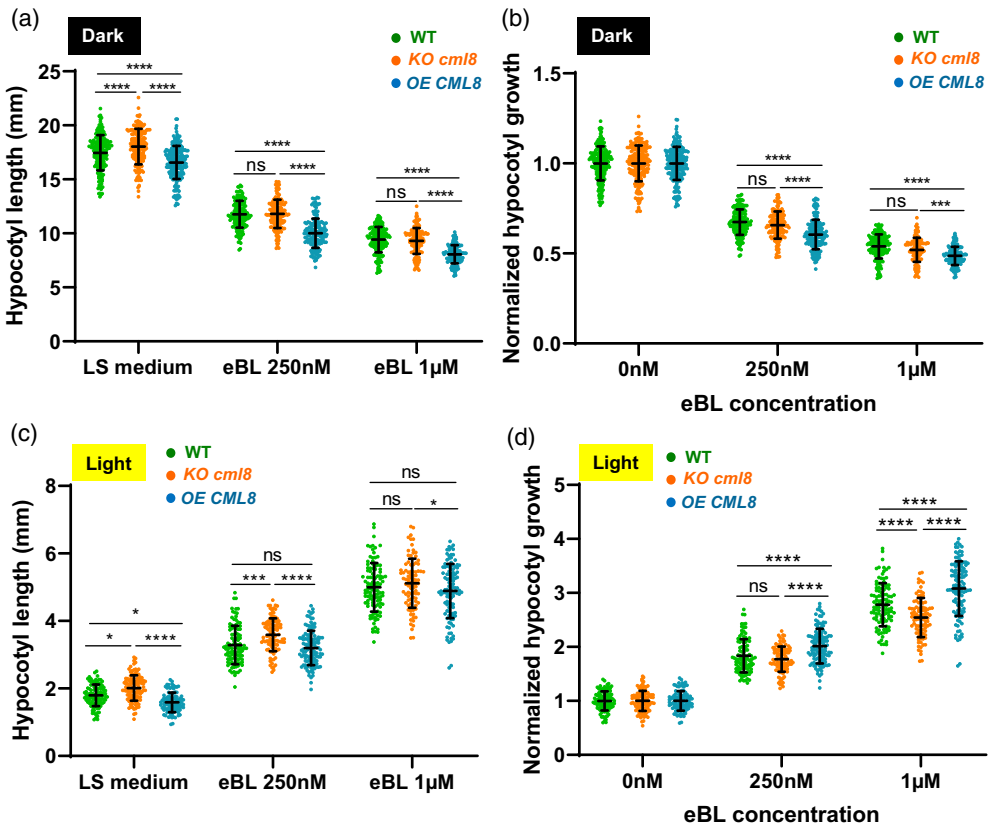

Figure 3. Effect of light exposure (+ vs. −) and brassinosteroid addition on hypocotyl elongation of mutant (KO *cml8* or OE *CML8*) or WT *A. thaliana* lines.
Quantitative analysis of hypocotyl elongation of the WT accession or mutants after culture in the dark (a, b) or in the presence of light (c, d) in response to eBL supply or not in the medium. Hypocotyl lengths of WT and *cml8* mutant seedlings grown on LS medium supplemented with eBL are shown relative to the standard culture condition (0 nM eBL). Data are presented for seedlings grown in the absence of light (b) and under light conditions (d).
Hypocotyl length was measured 5 days after germination induction for all genotypes grown on standard LS medium or medium supplemented with 250 nM or 1 µM eBL. Individual data points for each genotype are plotted. Black horizontal bars represent the means, and error bars represent the standard deviation. The data shown in (a) represent biological triplicates with 151–228 values per genotype/treatment combination; in (c), data represent biological triplicates with 90–119 values per genotype. Asterisks indicate significant differences between WT and *cml8* genotypes following two-way ANOVA with Tukey's multiple comparison test (*P* values are represented as follows: "****"<0.0001; "**"<0.01; "*"<0.05; and "ns": not significant).

Under standard condition (LS medium), the KO *cml8* line's average PR growth was 27% higher than the reference line (Figure 2b), whereas a significant reduction in PR growth was observed for the two OE *CML8* lines tested (Figure 2b; Figure S3a). The complemented line (*cml8.2_C#13*) shows the same level of growth as the WT under standard conditions (Figure S3c). Taken together, these data indicate that CML8 acts as a negative regulator of PR growth.

To test whether CML8 is involved in BR responses, we replicated these phenotypic analyses by transferring 5-day-old seedlings to LS medium supplemented with eBL concentrations known to inhibit root elongation: 50 and 500 nM (Clouse et al., 1996; Mussig et al., 2003). As expected, in response to exogenous eBL treatment, a concentration-dependent reduction in PR growth was observed in the WT line, reaching an average reduction of 46% at 500 nM when compared to medium devoid of eBL (Figure 2b,c). To highlight the effect of eBL treatment on the different genotypes, the data were normalized with the mean of the values of PR length obtained in standard growth condition for each genotype (Figure 2c). According to the normalized data, the KO line did not show an altered response to exogenous supply of eBLs, whereas the root growth of OE lines was less significantly affected by the supply of eBLs than that of the WT (Figure 2c; Figure S3b).

CML8 has significant expression in the hypocotyl (Figure 1d), a structure whose elongation is finely regulated by the integration of light messages and hormonal signals (Lin et al., 2021; Tanaka et al., 2003). To evaluate the involvement of CML8 in this process, a comparative analysis of the behavior of the different lines was undertaken by measuring hypocotyl growth in the absence or presence of light (Figure 3; Figures S4 and S5). As expected, darkness stimulates hypocotyl growth in the WT line (Figure 3a). Interestingly, *cml8* mutant lines exhibit

contrasting phenotypes. The *cml8* knockout mutant (KO *cml8*) displays elongated hypocotyls, whereas overexpression lines (OE *CML8*) have significantly shorter ones (Figure 3a; Figure S4a). The complemented mutant line no longer showed any significant difference in hypocotyl elongation in the dark (Figure S5a), which means that CML8, as at the root level, negatively regulates Arabidopsis hypocotyl growth under conditions of skotomorphogenesis.

To explore the involvement of CML8 in the sensitivity to BRs, we similarly reproduced the hypocotyl elongation experiment, supplementing the medium with 250 nM and 1 μM eBL (Figure 3a,b; Figures S4a,b, and S5a,b). Light and BR oppositely control the developmental switch from skotomorphogenesis in the dark to photomorphogenesis in the light (Lin et al., 2021; Nakamoto et al., 2006). Under *in vitro* conditions, it has been reported that the exogenous supply of BR has a stimulatory effect on hypocotyl growth of light-grown seedlings, but an inhibitory effect on hypocotyl elongation in the dark (Turk et al., 2003). As expected, eBL addition to the medium (both 250 nM and 1 μM) significantly reduced WT hypocotyl length by 33% and 46%, respectively (Figure 3a,b). The *cml8* KO and the complemented lines behaved similarly to the WT when eBL was exogenously applied (Figure 3b; Figure S5b). OE *CML8* lines exhibited reduced hypocotyl length under control conditions (Figure 3a), and exogenous eBL application significantly suppressed their elongation to a greater extent compared to WT and *cml8* KO genotypes (Figure 3b; Figure S4b).

We next explored how *cml8* genotypes behave in the presence of light, during photomorphogenesis, which is also known to be regulated by BRs. Light, in contrast to darkness, acts as an inhibitor of hypocotyl cell elongation, thereby reducing hypocotyl length (Lin et al., 2021). Indeed, we observed in all genotypes a reduction of more than 80% of the hypocotyl size in light versus dark conditions (Figure 3a,c). Under light conditions on LS medium, the OE *CML8* line displayed a significantly shorter hypocotyl compared to the WT and KO (Figure 3c). Conversely, the *cml8* knockout mutant showed significantly more elongated hypocotyls than the WT and OE *CML8* (Figure 3c). This phenotype is no more observed in the complemented line (Figure S5c), indicating that CML8 acts as negative regulator of plant cell growth in different organ and physiological conditions. In response to eBL treatments combined with light, an increase in hypocotyl growth was observed in all genotypes (Figure 3c,d; Figures S4c,d, and S5c,d). Interestingly, analysis of normalized data revealed a significantly greater increase in hypocotyl length for OE CML8 lines compared to the WT and KO *cml8* upon eBL application (both 250 nM and 1 μM). The increase was approximately 17% and 30% at these respective concentrations (Figure 3d; Figure S4d). The *cml8* knockout mutant displayed a significantly weaker stimulation of hypocotyl growth (~20%) at the high eBL concentration (1 μM) compared to the WT (Figure 3d). Notably, this differential response was abolished in the complemented line (*cml8.2_C#13*) (Figure S5d).

Collectively, these data illustrate that *CML8* overexpression enhances eBL sensitivity and that CML8 acts as a negative regulator of cell elongation in both PR and hypocotyl tissues. Furthermore, altered BR sensitivity in *cml8* lines indicates that *CML8* expression level (knockout vs. overexpression) can modulate physiological responses by affecting BR signaling, BR homeostasis, or potentially both.

CML8 loss and gain of function impacts expression of genes associated with plant growth and development

To specify the functions that CML8 regulates in early seedling development, we carried out a comparative global transcriptomes analysis of the *cml8* lines (OE and KO) compared to WT. We observed 2696 differentially expressed genes (DEGs) between the WT and the KO *cml8* (Figure 4a), and almost 6-fold fewer (401 DEGs) when comparing the *CML8* overexpressing line to the WT (Figure 4b). Among this list of DEGs (Data S1 and S2), 1627 genes are upregulated and 1069 are downregulated in the KO (Figure 4a). For the overexpressing line, 126 genes are more highly expressed compared to the WT and 275 genes are less expressed than in the WT (Figure 4b). The induction of a large number of genes (n = 1627) in the KO line suggests that CML8 might function primarily as a negative regulator, consistent with the root and hypocotyl growth phenotypes we observed. To gain a better insight into the biological significance associated with those DEGs, we carried out a GO biological process enrichment analyses on our DEG lists using DAVID (the Database for Annotation, Visualization, and Integrated Discovery, https://david.abcc.ncifcrf.gov/, v2022q2) (Huang da et al., 2009; Sherman et al., 2022) (Figure 4c,d). In the *cml8* KO mutant, a clear enrichment was found for biological processes such as growth, differentiation, development as well as for processes associated with them such as biogenesis and plant cell wall modifications or microtubules-associated movements (Figure 4c, upper panel). Among the downregulated genes, the enriched functional classes were related to a range of categories that are defined in the response to stimuli (hypoxia, light, salt …) (Figure 4c, lower panel). In the gain-of-function line, OE *CML8*, fewer genes were induced, but statistical analyses show a significant enrichment for GO categories that are associated with growth, development, and BR responses, with a 10-fold enrichment (Figure 4d, upper panel). Regarding downregulated genes in OE *CML8*, functional classes that are linked to responses to biotic and abiotic stresses were over-represented (Figure 4d, lower panel). These global analyses indicate that CML8 impacts the expression level of genes

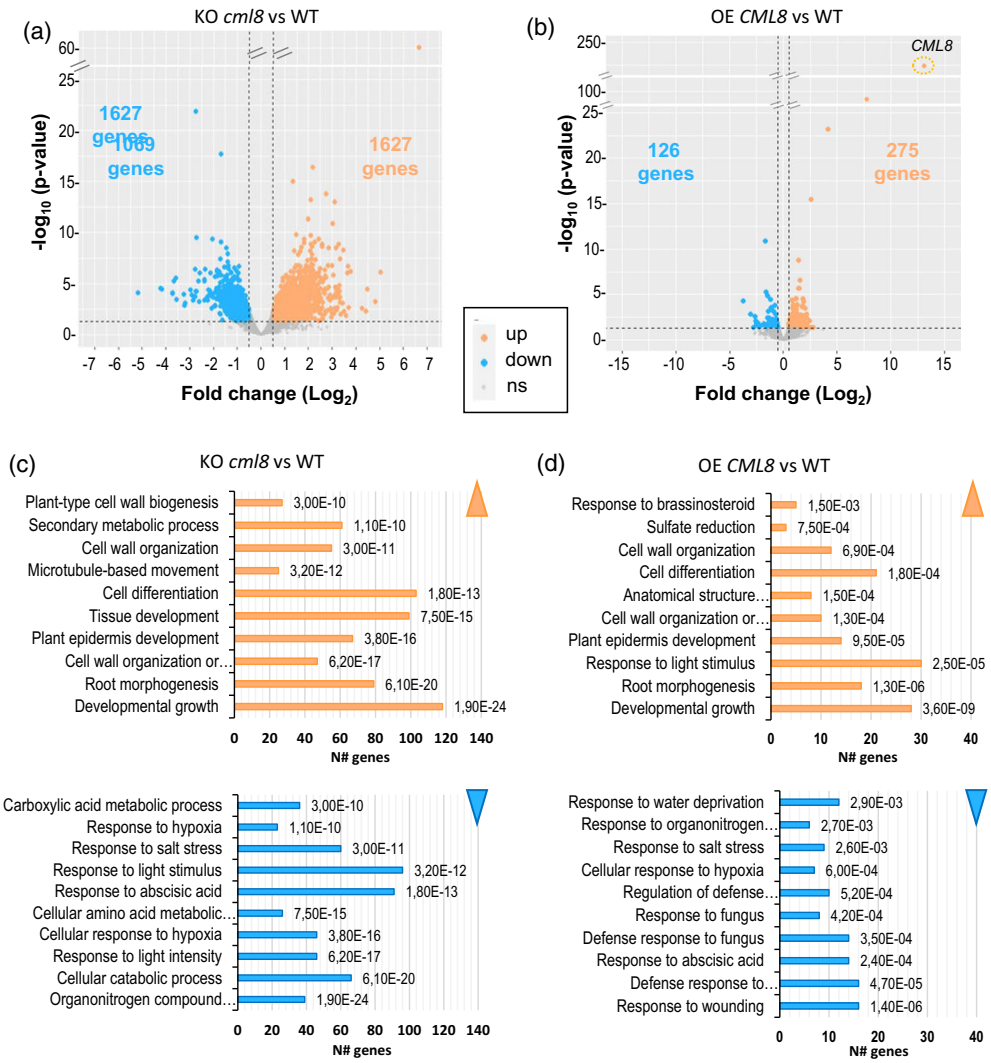

Figure 4. RNA-Seq analysis of genes whose expression is modulated by CML8 in *A. thaliana* seedlings.
7-day-old seedlings of the three reference genotypes (WT, KO *cml8*, OE *CML8*) grown *in vitro* were used to perform transcriptome analyses by RNA-Seq. Comparative analyses of the data obtained in the WT and *cml8* genotypes are displayed as volcano plots (a, b) which allow the quantitative description of the number of genes that are significantly differentially expressed (DEGs) compared to the WT in the KO *cml8* (a) and in the OE (b). A gene was considered (i) differentially expressed if its adjusted *P* value ≤0.05 and (ii) upregulated (orange) with a fold-change $Log_2FC \geq 0.5$ or downregulated (blue) with a fold-change $Log_2FC \leq -0.5$.
(c, d) The results of the GO (Gene Ontology) Biological Process (BP) enrichment analysis are illustrated. The search was performed for DEGs that were induced or repressed in the KO *cml8* (c) and OE (d) using DAVID bioinformatics resources (Huang da et al., 2009; Sherman et al., 2022). Only the top 10 results were retained for illustration.

associated with growth and development and highlight a particular link with the BRs pathway.

CML8 regulates the expression of BR-responsive genes

As we have previously established a link between CML8 and the BR pathway, we then compared the DEGs obtained in the *cml8* mutant lines to a list of BR-responsive genes generated by Chaiwanon and Wang (2015) through a set of RNAseq data (Chaiwanon & Wang, 2015). Remarkably in both KO *cml8* and OE, almost 40% of the DEGs (i.e., 1123 genes) are reported to be BR-responsive genes (Figure 5a). This is a significant enrichment (almost 3-fold) since only about 14% of genes in the *A. thaliana* genome (TAIR 10.1) are predicted to be BR-sensitive. This illustrates that the modulation of *CML8* expression greatly impacts the expression level of many BR-regulated genes.

In the model plant *A. thaliana*, two key transcription factors, BZR1 and BES1, are implicated in the BR regulation during plant development in the BRI1-regulated pathway (Kim & Wang, 2010). To go further, we searched for genes directly regulated by BZR1 and BES1 by comparing BR-responsive DEGs to the lists of BES1 and BZR1 target

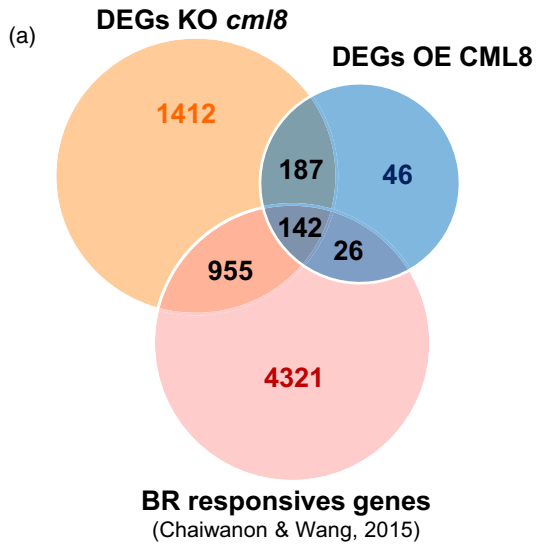

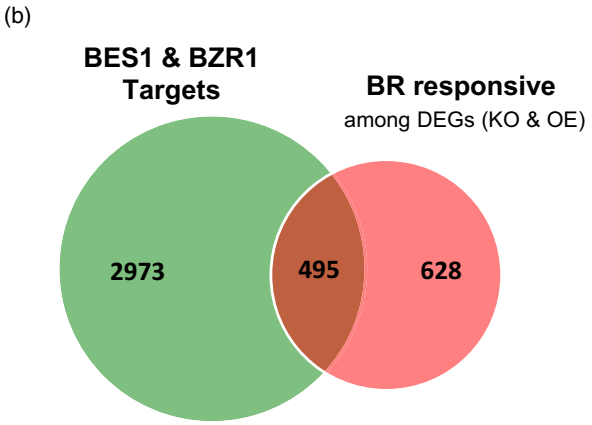

(c)

	Gene ID	Gene Name	target of …	logFC (ko *cml8* vs WT)	FDR
BRASSINOSTEROID Related	AT4G32910	**SBB1** (SUPPRESSOR OF BAK1)	-	-0,662	5,17E-03
	AT4G31910	**BAT1** (BR-RELATED ACYLTRANSFERASE 1)	BZR1	1,209	1,81E-02
	AT3G50660	**DWARF4** /DWF4	BZR1	0,609	2,36E-02
	AT2G03760	**SOT12**/AtST1 (SULPHOTRANSFERASE 12)	BZR1	-0,805	2,38E-02
AUXIN Related	AT1G56220	Auxin-Repressed Protein	BZR1	-0,997	6,76E-04
	AT2G38120	**AUX1** (AUXIN RESISTANT 1)	BZR1	0,531	2,62E-02
	AT5G43890	**YUCCA5** (YUCCA-like flavin monooxygenase)	-	0,993	3,24E-02
	AT5G50760	**SAUR55** (SMALL AUXIN UPREGULATED RNA 55)	BZR1	1,919	2,26E-06
	AT4G38860	**SAUR16** (SMALL AUXIN UPREGULATED RNA 16)	BZR1	0,801	3,05E-02

	Gene ID	Gene Name	target of …	logFC (ko *cml8* vs WT)	FDR
CELL EXPANSION	AT5G39860	**PRE1** (PACLOBUTRAZOL RESISTANCE1).	-	1,846	3,55E-04
	AT1G19900	**RUBY** (Secreted Galactose Oxidase)	BZR1	3,174	3,23E-05
	AT4G30290	**XTH19** (XYLOGLUCAN ENDOTRANSGLUCOSYLASE/HYDROLASE 19)	BES1	3,107	2,69E-03
	AT4G03210	**XTH9** (XYLOGLUCAN ENDOTRANSGLUCOSYLASE/HYDROLASE 9)	BZR1	1,621	8,82E-07
	AT2G39700	**EXPA4** (EXPANSIN A4)	BZR1	0,822	7,28E-03
	AT2G20750	**EXPB1** (EXPANSIN B1)	BZR1	2,334	1,08E-04
	AT5G53250	**AGP22** (ARABINOGALACTAN PROTEIN 22)	-	3,146	2,26E-05
	AT5G65390	**AGP7** (ARABINOGALACTAN PROTEIN 7)	BZR1	1,331	1,34E-05
	AT1G53830	**PME2** (PECTIN METHYLESTERASE 2)	BZR1	2,150	2,04E-09
	AT1G02730	**CSLD4** (Cellulose Synthase-Like family D)	-	2,502	6,28E-06

Figure 5. CML8 participates in the control of numerous genes associated with plant growth and brassinosteroid regulation.
(a) Venn diagram shows overlaps between genes differentially expressed (DEGs) in *cml8* genotypes and brassinosteroid-responsive genes reported in the RNA-seq data from Chaiwanon and Wang (2015).
(b) Estimation of the number of direct targets of BES1 and BZR1 among DEGs in *cml8* genotypes identified as BR responsive. The study was conducted using the lists of BES1 and BZR1 target genes identified by CHIP-seq, respectively, reported by Yu et al. (2011) and Chaiwanon and Wang (2015).
(c) List of genes selected to illustrate the involvement of CML8 in the regulation of the expression of genes associated with hormone signaling ("brassinosteroid related" or "auxin related") or cell expansion processes. The AGI (Gene ID) and gene name (according to TAIR × annotation) are indicated as well as the induction values (Log_2FC) and FDR (an adjusted *P*-value to trim false-positive results). The column "Target of …" indicates whether the selected gene has been identified or not as a target of BZR1 or BES1.

genes experimentally obtained by chromatin immunoprecipitation sequencing (ChIP seq) approaches (Sun et al., 2010; Yu et al., 2011) and data compiled in Chaiwanon and Wang (2015). Based on these analyses, the proportion of genes that could be targets of BES1–BZR1 is estimated to 42%. In comparison, data compiled by Nolan *et al.* (2017) indicated that approximately 35% of the reported BR-responsive genes were putative targets of BES1–BZR1.

To identify the underlying mechanisms by which CML8 controls the development of Arabidopsis seedlings, we have identified through GO analyses that DEGs are clearly associated with plant growth control. These include players in the hormonal controls associated with BR or auxin pathways or related to cell expansion (Figure 5c). For the BR pathway, we noticed that genes associated with the BR biosynthetic pathway such as *DWARF4* (*DWF4*), the

rate-limiting enzyme of the biosynthetic pathway or genes associated with BR modifications and/or endogenous BR level such as *BAT1* and *SOT12* (*BR-related acyltransferase 1* and *sulphotransferase 12*) were deregulated in the KO (Choi et al., 2013; Marsolais et al., 2007; Tanaka et al., 2005). The crosstalk between BR and auxin being well documented, particularly in the context of cell elongation and photomorphogenesis (Lin et al., 2021; Oh et al., 2014; Wang et al., 2019), we next explored these auxin-regulated genes in more detail. Five marker genes of auxin signaling with differential expression profiles are reported (Figure 5c). YUCCA5 belongs to the family of YUC (or YUCCA) genes that encode monooxygenases that catalyze a key step in the auxin biosynthetic pathway (Challa et al., 2016). *YUCCA5* was upregulated in the KO *cml8* mutant, suggesting a possible increase in auxin response compared to the WT. This hypothesis was supported by the gene expression of the important SAUR (Small Auxin Upregulated RNAs) family described as early auxin response genes (Ren & Gray, 2015). SAUR55 and SAUR16 are indeed expressed more abundantly in the KO mutant as other members of the SAUR family (SAUR 20, 21, 22, 23, 24, and 31) (Data S1 and S2). Significantly, 80% of the identified auxin-responsive genes are known direct targets of BZR1 (Figure 5c), supporting the potential for crosstalk between the BR and auxin signaling pathways in CML8-mediated physiological processes. Given the findings of this study regarding CML8's role in root growth and hypocotyl elongation, we investigated its potential involvement in regulating the process of cell expansion. Both auxin and BRs participate in this control notably through ARF6 and BZR1 by regulating targets such as *PRE1* (*paclobutrazol resistant 1*), SAURs, or genes encoding for enzymes associated with cell wall remodeling (e.g., *XTH* and *expansin*) (Li et al., 2018; Oh et al., 2014). Intriguingly, those genes known to drive cell expansion displayed significantly higher expression levels in the *cml8* knockout mutant (Figure 5c, right panel). This finding supports the hypothesis that CML8 functions as a negative regulator of cell expansion, thereby influencing hypocotyl and root elongation. Collectively, these results suggest that dysregulation of cell expansion mechanisms in the *cml8* knockout mutant likely contributes to its enhanced growth under standard culture conditions.

CML8 interacts with the BR receptor BRI1 *in planta*

Due to the large number of genes directly linked to BR responses in *cml8* genotypes, we assumed that CML8 is likely involved in further upstream in the BR signaling pathway. Interestingly, a previous study using the intracellular part of the BRI1 receptor or a synthetic peptide proposed that different isoforms of the typical CaM (2, 4, 6, and/or 7) are able to interact *in vitro* with BRI1 and in particular with the BRI1 kinase subdomain VIa (Oh et al., 2012). In the same study, *in vitro* interaction tests with CML8 or CML9 were found to be negative, which raises questions about the situation *in planta* (Oh et al., 2012). To investigate the potential *in planta* interaction between BRI1 and CML8, we sought to perform co-immunoprecipitation experiments using transiently expressed, tagged protein constructs. However, we first ascertained that BRI1 and CML8 have a tissue expression pattern and a sub-cellular localization compatible with a physical interaction. The available transcriptomic data confirmed the compatible tissue expression patterns of *CML8* and *BRI1* in Arabidopsis, particularly at the root level (Figure S6). To gain a more detailed understanding of CML8 expression, we examined single-cell RNA sequencing data for Arabidopsis roots. Specifically, we analyzed those published by Nolan et al. (2023) and Shahan et al. (2022) using the online tool ARVEX (https://shiny.mdc-berlin.de/ARVEX/). This analysis revealed that *CML8* is most highly expressed in both trichoblasts and atrichoblasts throughout the root, as well as in the endodermis of the transition and elongation zones. *BRI1* shows a similar expression profile to *CML8* based on the same data set, particularly in epidermal cells.

Furthermore, the sub-cellular co-localization experiments of these two proteins after transient expression in *N. benthamiana* cells (Figure 6a–c) showed that, as expected, BRI1 is located at the plasma membrane and that CML8 has a nucleocytoplasmic distribution (Figure 6a,b). A fraction of CML8 could, therefore, interact with the cytoplasmic domain of BRI1, as suggested by the co-localization of both proteins highlighted by the fluorescent signal overlay (Figure 6c).

We then used co-immunoprecipitation (Co-IP) assays *in planta* to investigate the physical interaction between CML8 and BRI1 (Figure 6d; Figure S7). We transiently co-expressed CML8 tagged with HA and BRI1 tagged with mCitrine in tobacco leaves and subjected protein extracts to immunopurification of BRI1-mCitrine with anti-GFP antibodies (IP α-GFP) (Figure 6d; Figure S7).

We investigated the *in planta* interaction between BRI1 and CML8 under two physiological conditions (i) in the presence and (ii) in the absence of exogenously applied BRs (Figure 6d, Mock vs. eBL). This strategy aimed to determine whether BRI1 and CML8 interact within the plant and if BRI1 activation after ligand binding affects this interaction. For the control condition, leaves were infiltrated with water and incubated for 2 h before harvest. In the BR treatment condition, leaves were infiltrated with 1 μM eBL solution and incubated for 2 h before being harvested (Figure 6d,e).

In the control condition (mock), immunoprecipitation (IP) with anti-GFP antibodies successfully captured BRI1-mCitrine (Figure 6d, IP α-GFP). CML8-HA co-purified with BRI1-mCitrine in the IP fraction, indicating an

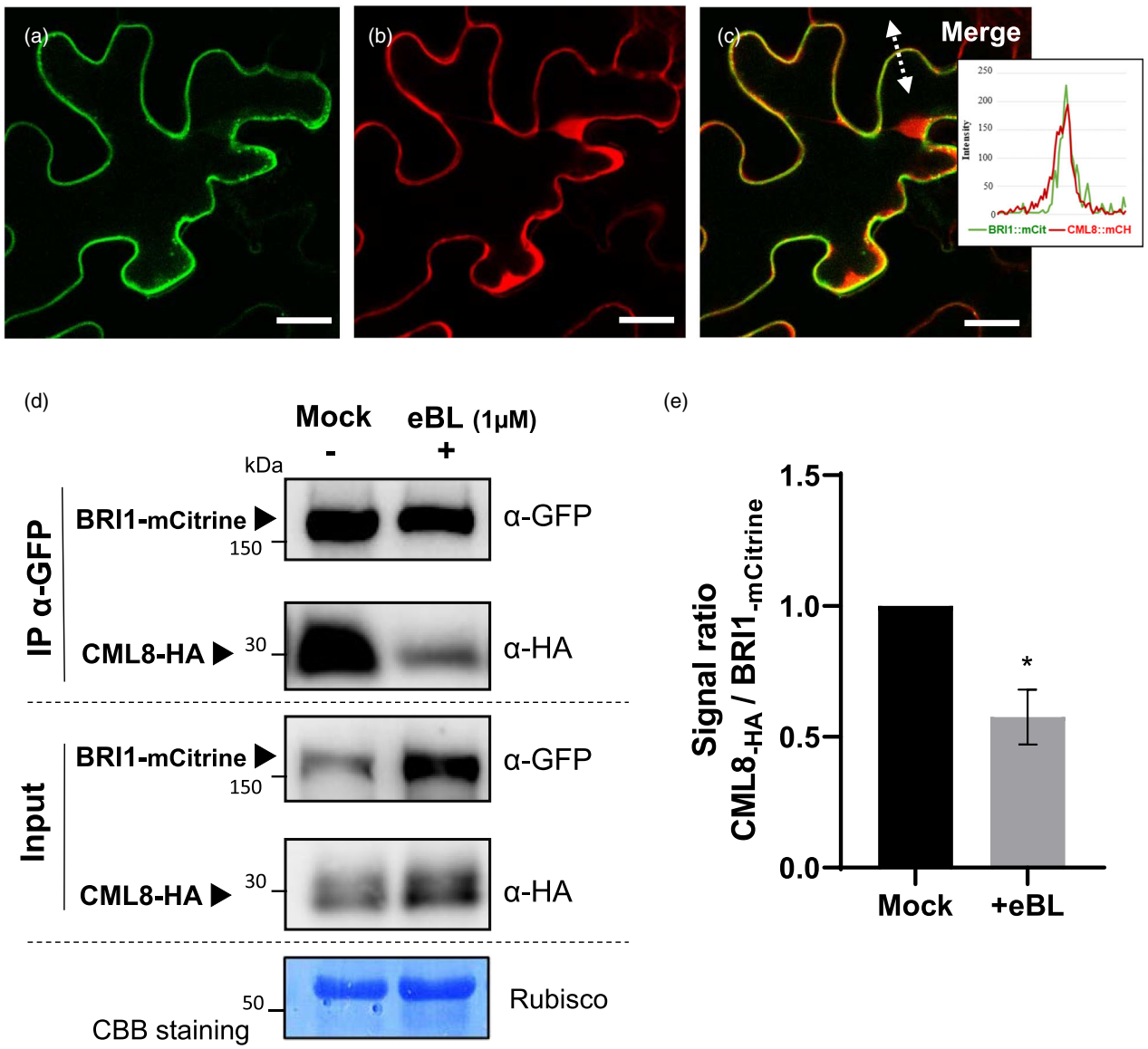

Figure 6. Transient co-expression of CML8 and BRI1 in *Nicotiana benthamiana* reveals *in planta* interaction *via* co-immunoprecipitation.
Sub-cellular localization of *pUbi10::BRI1-mCitrine* (a) and *pUBI10::CML8-mCHERRY* (b) by confocal microscopy after expression in *N. benthamiana* cells.
(c) Overlay of mCHERRY and mCitrine detection channels to assess possible co-localization of BRI1 and CML8. At the indicated arrow, fluorescence intensity quantification was performed with Leica Application Suite X and is shown in the insert box. The superposition of the fluorescence peaks of mCitrine and mCHERRY at the same location suggests a sub-cellular colocalization of the two fluorochromes in this area. Scale bars: (a–c) 24.22 µm.
(d) Co-immunoprecipitation (Co-IP) interaction assay between BRI1::mCitrine (159 kDa) and CML8::6HA (25 kDa) tagged proteins transiently expressed in *N. benthamiana* leaves. Leaves treated with 1 µM epibrassinolide (+ eBL) or water (Mock -) for 2 h. Co-IP was performed using anti-GFP antibodies able to recognize both GFP and one of its variant, the mCitrine. Total proteins from the crude extract (Input) and eluates (IP) were analyzed by Western blot using anti-GFP (α-GFP) and anti-HA (α-HA) antibodies. Protein (rubisco) detection by Coomassie Brilliant blue (CBB) is shown below the Western blots to assess protein loading on gels. The results shown here are representative of four independent biological replicates.
(e) Relative quantification of co-immunoprecipitated CML8 in the presence (+eBLs) or absence (–Mock) of eBLs. The intensity of the signals (BRI1 and CML8) used to make these comparisons was measured using the Image Lab 6.1 (Bio-Rad). The signal intensity of coimmunoprecipitated CML8 was quantified relative to the precipitated BRI1. The quantification results were obtained from four independent experiments and analyzed using a Mann–Whitney U test, a non-parametric test (significant differences between the treatments are indicated by asterisks *P value = 0.0286).

interaction between these proteins *in planta* (Figure 6d). As expected, co-expression of GFP alone with CML8-HA followed by GFP immunopurification did not result in CML8-HA co-purification (Figure S7a), demonstrating the specificity of the BRI1–CML8 interaction. Then, we investigated the effect of ligand binding on this interaction (Figure 6d, lane +eBL). Four independent Co-IP experiments revealed a decrease in CML8-HA co-purified with BRI1-mCitrine upon eBL treatment compared to controls (Figure 6d). Western blot quantification (n = 4) confirmed a

significant 40% reduction in CML8 co-precipitated with BRI1 in the presence of exogenous BRs (Figure 6e). These results suggest that CML8 interacts more efficiently with, or within a complex where, BRI1 is not fully activated. Conversely, BR application might limit BRI1–CML8 interaction or trigger CML8 release from the initial complex.

To assess the specificity of the BRI1–CML8 interaction, we employed co-immunoprecipitation with additional Ca^{2+} sensor proteins from *Arabidopsis*. The "typical" CaM, CaM2, shares considerable similarity with CML8, including comparable size and four calcium-binding motifs, with a 73% protein sequence identity. Conversely, CML42 is highly distinct, exhibiting only 35% and 39% identity with CaM2 and CML8, respectively. Co-IP experiments revealed co-precipitation of both CML8 and CaM2 with BRI1 (Figure S7b), suggesting their potential interaction with the receptor. In contrast, no significant signal was detected for CML42 even with extended Western blot exposure (Figure S7b), indicating a possible lack of interaction between CML42 and BRI1.

cml8 mutations affect BES1 regulation and the transcriptional control of genes involved in BR homeostasis and signaling

To elucidate the functional consequences of the BRI1–CML8 interaction, we investigated the impact of *CML8* expression on established molecular and biochemical markers of the BR signaling pathway in *cml8* knockout (KO) and overexpression (OE) genotypes. We evaluated the phosphorylation status of BES1 to assess BR signaling activity. BES1 is a transcriptional regulator and its activity is negatively regulated by phosphorylation. The non-phosphorylated form ("BES1") acts as a positive regulator of BR signaling by binding to promoters of BR-regulated genes, while in the absence of BRs, BES1 accumulates under its inactive phosphorylated version ("pBES1") (Yin et al., 2002). The BES1/pBES1 ratio is a commonly used indicator of the activation level of BR signaling (Yin et al., 2002). Using an anti-BES1 antibody, the two states of phosphorylation of BES1 are detectable through Western blot analysis and the proportions of each form can be estimated (Figure 7a). The BES1/pBES1 ratio in the OE *cml8* line exhibited a trend of higher values compared to both WT and *cml8* KO plants (Figure 7b). This difference was statistically significant between KO and OE lines, suggesting a potential association between *CML8* overexpression and enhanced BR signaling activity under standard growth conditions (Figure 7b). These findings support a potential positive correlation between CML8 abundance and activation of the BR pathway, consistent with the observed hypersensitivity to BRs (Figure 3).

To further explore this hypothesis, we performed quantitative real-time PCR (RT-qPCR) analyses to measure the expression levels of known BES1/BZR1 target genes involved in BR signaling, biosynthesis, or catabolism (Figure 7c; Figure S8). We first studied the expression of the *SAUR15* (*SMALL AUXIN UPREGULATED RNA 15*) gene known to be positively regulated by BES1 (Yin et al., 2005). The *cml8* knockout line displayed a significant decrease in *SAUR15* expression (Figure 7d). We further investigated the expression of genes involved in BR biosynthesis and catabolism in *cml8* lines compared to the WT. BR biosynthesis genes *DWF7*, *DWF4*, and *CPD* exhibited significantly higher expression in the *cml8* KO line (Figure 7e). Conversely, the overexpression of *CML8* (OE *CML8*) resulted in a significant downregulation of *DWF7* and *CPD* compared to the WT (Figure 7e). Because the BR biosynthetic pathway is inhibited by BRs as part of a negative feedback (Yu et al., 2011), these results are consistent with the hypothesis that the BR signaling is activated by CML8. We also examined the profile of *BAS1* (*PHYB-4 activation-tagged suppressor1*) which encodes a cytochrome P450 monooxygenase (CYP72B1/CYP734A1) able to inactivate BRs and modulate photomorphogenesis (Neff et al., 1999). *BAS1* expression was very low in OE *CML8* line compared to KO or WT (Figure 7f), indicating that BR homeostasis could therefore be influenced by CML8. The time-course expression profiles of these genes following eBL application (1 μM) were analyzed in the different *cml8* lines (Figure S8). The eBL application suppresses the expressions of *DWF4*, *DWF7*, and *CPD* over time in the WT line. The *cml8* KO line showed much lower levels of expression of these genes, suggesting increased sensitivity to eBL (Figure S8a). Conversely, *BAS1* expression increased upon eBL treatment in the overexpressor line, whereas the mutant mimicked the WT response (Figure S8b). Finally, 3–6 h after eBL application, BR signaling, as exemplified by the *SAUR15* marker, is more strongly induced in the *cml8* KO mutant (Figure S8c).

Our functional analyses link CML8 to the regulation of root growth and hypocotyl elongation in Arabidopsis. RNA-seq and RT-qPCR data further suggest CML8's connection to genes involved in growth and BR signaling. Additionally, *in planta* interaction with the BR receptor BRI1, BES1 phosphorylation, and transcriptional profiling all provide evidence supporting CML8's regulatory function within the BR pathway.

DISCUSSION

In a fluctuating environment, modulation of plant growth and/or development is essential for plant survival. At the earliest stages of plant development, the control of cell expansion is found to be a tightly regulated process at the crossroads of multiple controls exerted by light, temperature, and several phytohormones (Vanstraelen & Benkova, 2012). Here, we provide molecular and physiological evidence that CML8, a calcium signaling actor, plays a role in the modulation of BR-related signaling pathways that contribute to the regulation of root and hypocotyl growth of

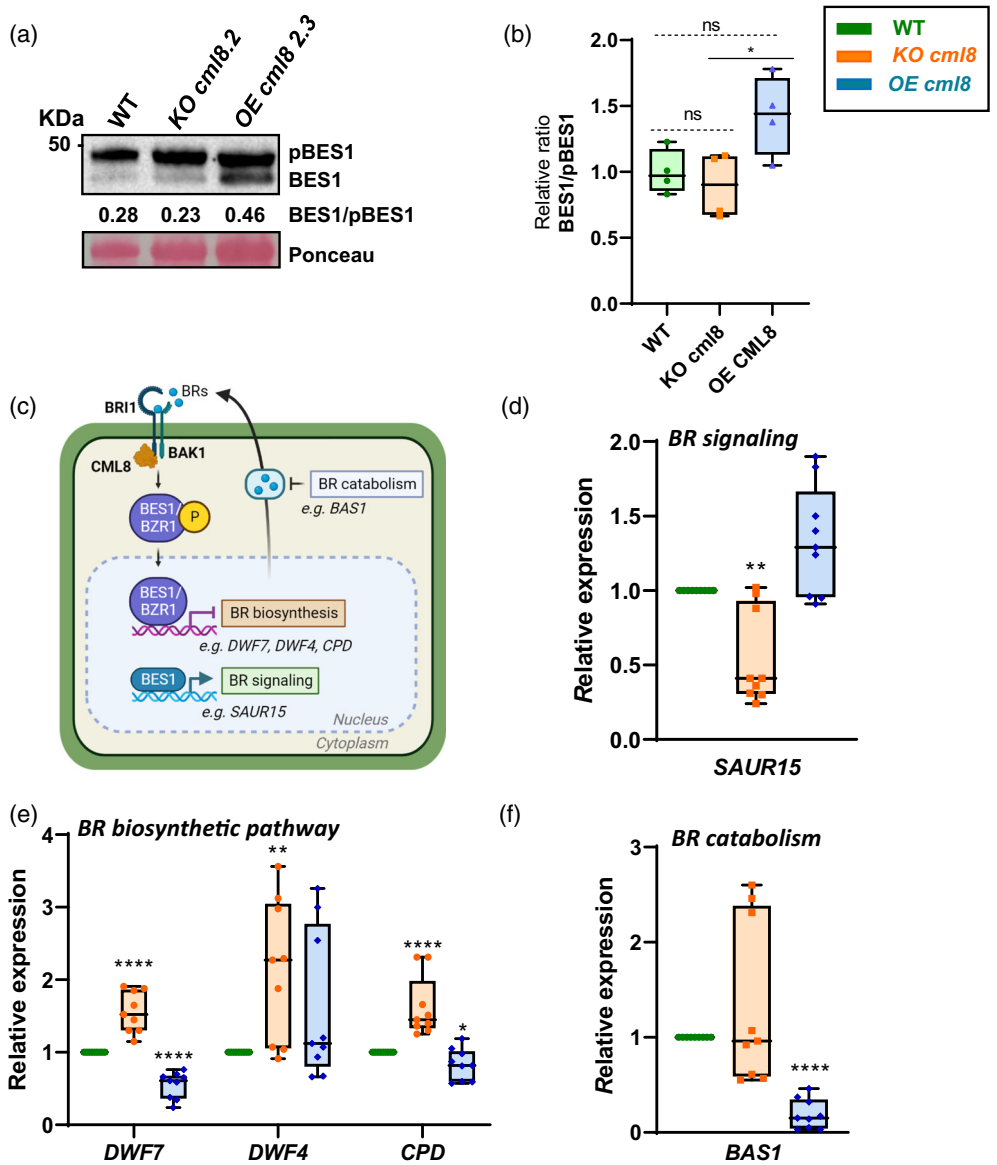

Figure 7. CML8 alters the brassinosteroid signaling pathway.
(a) Illustration of the phosphorylation status of BES1 in the WT (Col8) and *cml8* mutant lines (KO *cml8.2* or *OE CML8*). Western blot is representative of four biological replicates.
(b) Quantitative analysis of the phosphorylation status of BES1. Following pooling of the four biological replicates, the phosphorylation status of BES1 was quantitatively analyzed. One-way ANOVA was performed to compare the BES1 phosphorylation levels between the lines of interest. Significant differences are indicated by asterisks (*$P < 0.05$), and "ns" denotes not significant.
(c) Simplified scheme of the signaling associated with the perception of BRs that leads to genetic reprograming. The positioning of BES1 and the actors analyzed by RT-qPCR are shown.
(d–f) Relative expression of brassinosteroid-responsive genes in WT and *cml8 Arabidopsis* lines (7-day-old seedlings) under standard conditions.
(d) *SAUR15*, a direct target of the transcription factor BES1. In (e), a sterol biosynthesis gene (*DWF7*) and two BR biosynthesis genes (*DWF4* and CPD), and finally (f) *BAS1*, a gene encoding an enzyme responsible for the degradation of active forms of brassinolides. The results presented are from the biological triplicate analysis. Error bar = standard error of the mean. Statistical analysis was performed using a Wilcoxon–Mann–Whitney test (*P* value "****"<0.0001; "**"<0.01; "*"<0.05; $n = 9$ at least for each line and each gene analyzed).

seedlings. All the biochemical and molecular analyses shed light on the biological significance of the interaction between BRI1 and CML8. Indeed, the interaction of CML8 with BRI1 and the effects of this interaction could account for many of the altered responses in *cml8* mutants including changes in the expression levels of BR-regulated genes, many of which are dependent on the transcription factors BES1 or BZR1. Ultimately, these alterations which

may affect the signaling or homeostasis of BRs could be associated with and explain the developmental phenotypes described for *cml8* mutants (Figures 2 and 3).

CML8 acts as a regulator of cell elongation during seedling growth

Analyses of *CML8* gene expression show a specific (although not exclusive) profile at the seedling stage, with expression identified in growing structures such as hypocotyls and PR. By using loss-of-function KO mutant for *CML8*, corresponding complemented line, and two independent overexpressor lines, we explore the significance of this profile. Interestingly, we have shown (Figures 2 and 3) that, in the absence of any treatment under standard culture conditions, the *cml8* lines show altered growth phenotypes when compared to the WT. Both root and hypocotyl growth measurements in the dark indicate that CML8 acts as a negative regulator of growth. The dark-positive (Figure 3a) or light-negative (Figure 3b) hypocotyl growth controls were found to be enhanced in *cml8* KO with different growth rates from those of WT. This suggests that controls of these processes are deregulated in the KO background. To identify the underlying mechanisms, we performed an expression analysis of transcriptome changes in *cml8* lines by RNAseq. The results obtained support that CML8 acts as a negative regulator of growth since numerous genes associated with growth-related biological processes are induced in the *cml8* mutant (Figures 4c and 5c). Intriguingly, a substantial proportion of the biological processes disrupted in *cml8* mutant backgrounds are linked to plant cell wall modifications, encompassing biogenesis, organization, and potentially other aspects. Notably, cell wall extensibility is a well-established factor regulating cell elongation, which underpins root and hypocotyl growth. BRs have been demonstrated to contribute to these responses (Ackerman-Lavert & Savaldi-Goldstein, 2020).

The involvement of CML8 in seedling growth is likely mediated by BRs

CML8 is tightly regulated both spatially and temporally by exogenous BR application (Figure 1), corroborating published transcriptomic data (Chaiwanon & Wang, 2015; Clark et al., 2021; Goda et al., 2004). Interestingly, while *CML8* expression is higher in lines with constitutively active BES1 and BZR1 compared to the WT (Figure 1d), available data do not indicate that *CML8* is a direct target of these regulators (Chaiwanon & Wang, 2015, Clark et al., 2021, Goda et al., 2004). A recent study by Kim et al. (2024) identified *CML8* as coregulated by BRs and BEH2 (BES1/BZR1 Homolog 2) but not by BZR1, similar to the regulatory profile of BAS1 (Kim et al., 2024). These findings suggest that CML8 might participate in a complex signaling pathway. Transcriptionally regulated by BR levels, it might also regulate downstream responses in a feedback loop.

BRs regulate the growth of the PR and hypocotyl of young seedlings by interacting with auxin signaling and light perception pathways (Zhu et al., 2013). The exogenous application of BRs is described to inhibit the growth of the PR, whereas the effect on the growth of the hypocotyl and cell elongation is light-dependent (Tanaka et al., 2003). We evaluate the behavior of *cml8* and WT genotypes in response to exogenous supply of BRs (i.e., eBL from 50 nM to 1 μM) (Figures 2 and 3). Root growth analysis revealed that eBL application abolished the differential response observed in the *cml8* KO line, causing it to resemble the WT phenotype. Conversely, the overexpressing lines exhibited enhanced root growth at 500 nM eBL (Figure 2c). This may be attributed to a diminished responsiveness of the OE to eBL application. Notably, the eBL concentrations used have been previously documented to significantly inhibit root growth. In roots, the function of BRs is complex, with a role in the control of elongation but also on many other processes including root meristem activity (Ackerman-Lavert & Savaldi-Goldstein, 2020; Vukasinovic et al., 2021; Wei & Li, 2016). Indeed, the regulation of elongation is BR-dose dependent since supplementation with low BR promotes root growth, whereas high BRs inhibit root growth (Clouse et al., 1996; Mussig et al., 2003). Some of those growing processes depend on BRI1 and its expression in the root epidermal cells (Wei & Li, 2016). For example, the short root phenotype of the BR-insensitive *bri1-116* mutant is suppressed by low concentrations of BRs (Gonzalez-Garcia et al., 2011). Thus, the responses observed upon eBL treatment in *cml8* genotypes could be explained both by differences in the level of endogenous BRs and by different threshold of sensitivity to the treatment.

BRs play crucial roles in regulating plant cell growth and morphogenesis, particularly in hypocotyl cell elongation (Clouse & Sasse, 1998; Delesalle et al., 2024). Endogenous BRs are necessary for normal *Arabidopsis* hypocotyl growth in both photomorphogenetic and skotomorphogenetic programs (Tanaka et al., 2003). This work revealed that *cml8* KO line displayed enhanced hypocotyl elongation under dark conditions (Figure 3a). However, exogenous application of eBL abolished this phenotype, resulting in a response similar to the WT line (Figure 3b). This suggests that the *cml8* KO might possess altered sensitivity to endogenous BR levels, which at these basal concentrations could promote hypocotyl growth. This hypothesis is consistent with the report that darkness activates BR signaling and hypocotyl growth by changing the abundance of BZR1 (Kim et al., 2014). Moreover, it has been shown that the application of high concentrations of BRs or the hypersensitive *bzr1-1D* mutant resulted in shorter hypocotyls (Zhang et al., 2015). Collectively this indicates that a very fine regulation of hypocotyl elongation of seedlings in the dark can take place due to the BR

concentrations present. BR signaling plays a key role in inhibiting hypocotyl elongation during the shade-to-light transition in seedlings. However, exogenous BR application can counteract this effect, promoting growth in light-grown seedlings (Tanaka et al., 2003). Interestingly, *cml8* mutant lines exhibited a contrasting response to BR treatment under light conditions compared to the WT. The *CML8* overexpressing lines exhibited enhanced hypocotyl growth, while the KO *cml8* line displayed reduced growth compared to WT (Figure 3d). Collectively, these results suggest a positive regulatory role for CML8 in BR signaling pathways during light-mediated hypocotyl elongation.

CML8 interacts with BRI1 and regulates downstream BR signaling cascade

Our findings suggest that CML8 functions as a negative regulator of both PR cell elongation and hypocotyl growth, potentially acting through a BR-dependent pathway. BRs exert diverse regulatory effects depending on their endogenous concentrations, with negative effects on root growth and skotomorphogenesis but with positive effects on growth in the light. Transcriptome profiling (RNA-seq) analyses of seedlings grown under standard conditions revealed that *CML8* expression levels (i.e., KO and OE lines) are associated with the modulation of a significant number of genes involved in BR signaling (Figure 5). A striking enrichment of BR-responsive genes (~40%) among the genes misregulated is revealed in *cml8* genotypes. ChIP-Seq data further indicated that 44% of these genes are directly regulated by the transcription factors BES1 or BZR1 (Figure 5a). These observations establish a direct link between CML8 and BR signaling. *cml8* mutant backgrounds exhibit altered expression of numerous genes involved in plant cell growth regulation, including those associated with auxin synthesis or signaling. This observation suggests a potential crosstalk between CML8 and auxin signaling pathways (Figure 5c). Auxin and BRs stimulate cell expansion and may act synergistically to promote hypocotyl elongation (Nemhauser et al., 2004; Tanaka et al., 2003). Beyond cell expansion, the auxin-BR crosstalk also involves auxin stimulation of BR biosynthesis through the induction of *DWARF4* which encodes a key enzyme in BR biosynthesis (Chung et al., 2011). The promotion of hypocotyl elongation by BR and BZR1 requires ARF6/8 (Tian et al., 2017). Moreover, transcriptomic and ChIP-Seq analyses reveal extensive overlap in target genes between ARF6/8, BZR1, and the light-regulated transcription factor PIF4, suggesting shared regulatory elements (Chaiwanon & Wang, 2015; Li et al., 2018; Oh et al., 2014).

This study positions CML8, a calcium sensor, as a potential regulator of BR signaling and developmental processes. Notably, calcium signaling has been previously linked to the BR pathway through its role in regulating BR biosynthesis. DWARF1, a key enzyme in early BR biosynthesis, has been identified as a Ca^{2+}/CaM-BPs (Du & Poovaiah, 2005). Du and Poovaiah (2005) demonstrated that DWARF1 requires interaction with CaM for *in planta* activity, highlighting the crucial role of calcium signaling in BR biosynthesis. Their unpublished data (cited in Du & Poovaiah, 2005) further suggest similar CaM interactions with other BR pathway enzymes like DWARF4 and CPD, indicating a more intricate calcium-mediated regulation of this pathway.

CML8 likely acts upstream in BR signaling, potentially *via* interaction with the main BR receptor BRI1. Based on our findings and those of Oh et al. (2012), BRI1 interaction appears restricted to ubiquitous plant CaMs or closely related CMLs, suggesting a potential role for specific Ca^{2+} sensor in BRI1 regulation. The ability of CML to interact with BRI1 is not shared by all CMLs, as demonstrated by the lack of binding observed with CML42 (Figure S7). The CML family is diverse in terms of protein size, number of Ca^{2+}-binding motif, and expression profile (Zhu et al., 2015). Despite biochemical similarities to typical CaM (McCormack & Braam, 2003; Zielinski, 2002), CML8 exhibits a distinct functional identity due to its unique spatiotemporal expression in seedlings, growing tissues, and roots (Figure S1), which have facilitated functional analyses and revealed a role in BR-dependent development.

Co-IP experiments have also revealed that ligand-activated BRI1 exhibits weaker interaction with CML8 (Figure 6d,e). This might be due to BRI1 intracellular domain phosphorylation events triggered by ligand binding and BRI1-BAK1 complex activation (Li et al., 2017). The BIR2/LRR-RLK model exemplifies ligand-dependent interactions. Indeed, BIR2 (BAK1-Interacting Receptor-like Kinase 2) negatively regulates flg22 responses by controlling BAK1 association with FLS2 in an inactive state. Ligand binding (PAMPs or BRs) triggers BIR2 release, allowing BAK1 recruitment to the activated receptor (Halter et al., 2014). Alternatively, CML8 might interact with the resting state of BRI1, and activation could trigger CML8 post-translational modifications (PTMs) (e.g., phosphorylation) that alter binding affinity. Supporting this, CaMs exhibit documented instances of interaction regulation through PTMs. Notably, CaM interactions with the epidermal growth factor receptor in animals are known to be modulated by phosphorylation (Villalobo, 2023). Ca^{2+} may further modulate CML8–BRI1 interaction. BR application (100 nM to 1 μM eBL) can elevate intracellular Ca^{2+} levels (Zhao et al., 2013). CaM–CaM-BP interactions can be either Ca^{2+}-dependent or -independent (Chin & Means, 2000). While Oh et al. (2012) demonstrated Ca^{2+}-dependence for BRI1 interaction with typical CaMs *in vitro*, the effect on CML8 interaction remains to be elucidated. Further studies are necessary to elucidate whether Ca^{2+} similarly affects BRI1's interaction with CML8. Moreover, we propose that CML8 interaction with BRI1 could modulate BR signaling

through the transcriptional regulation mediated by BZR1 and BES1. Upon activation, BES1 and BZR1 transcription factors act either as positive or negative regulators of BR-responsive genes involved in plant cell elongation (e.g., *PRE1*, *EXP*, and *SAURs*) and BR homeostasis.

In *Arabidopsis*, CML8 modulates BR biosynthesis and signaling, regulating hypocotyl elongation and PR growth. Further studies are required to dissect the molecular underpinnings of CML8 function, particularly its interaction with BRI1 and the downstream effects on BR signaling.

EXPERIMENTAL PROCEDURES

Plant material and growth conditions

Arabidopsis thaliana accession Columbia-8 (Col-8) served as the WT reference for all analyses. CML8 function was investigated using two 2 lines that overexpressed (*p35S::CML8*$_{CDS}$) the coding sequence of *cml8* gene (OE CML8 and OE CML8 3.2 in Figures S3 and S4) previously characterized by Zhu et al. (2017). Additionally, a T-DNA insertion line (SALK_022524C), designated "KO *cml8*," was used and characterized in this study (Figure S2). The absence of *CML8* transcript in KO *cml8* was confirmed by RT-qPCR (Figure S2b). To complement the KO line, transgenic lines were generated by reintroducing the *CML8* genomic sequence under its native promoter in the pGWB413 vector (Figure S2c). The *cml8.2_C#13* line used here displayed CML8 expression closest to WT levels (Figure S2c). CML8 expression in seedlings was monitored using a previously generated and described reporter line expressing the *CML8 promoter::uidA* fusion (Zhu et al., 2017). Mutants associated with BR signaling (*bes1-D* and *bzr1-1D, Col-0 background*) were already characterized by Ibanes et al. (2009) and Wang et al. (2002), respectively. The seeds used were from mother plants grown under the same conditions, over the same period, and the seeds were stored in the same conditions after harvest. The analyses were performed on seedlings grown *in vitro*. Seeds were surface sterilized and then sown on agar media (1.4% agar) containing Linsmaier and Skoog (LS) medium (0.5X) (Duchefa Biochemie, Haarlem, the Netherlands) supplemented or not with eBLs (Merck, Darmstadt, Germany). The plates were incubated for 2 days in the dark at 4°C to lift any residual seed dormancy and then transferred to a phytotron at 20/22°C with a 16-h photoperiod and 40% humidity. In the case of root phenotyping, although the plates were exposed to a photoperiod, the root system of the seedlings was not exposed to light as recommended by Dubrovsky and Forde (2012). For transient expression experiments, *Nicotiana benthamiana* plants were used for leaf agroinfiltration experiments as described by Lindbo (2007). The plants were grown in a phytotron at 25°C, with a 16-h/8-h photoperiod and a humidity of 60%. The tobacco plants were infiltrated 4 weeks after sowing.

Quantification of PR growth and hypocotyl elongation

In each experiment, 5–6 seedlings per lines were placed in the same plate under a given condition, and at least five culture dishes were prepared for a given condition. For the analysis of PR growth, 5-day-old seedlings were transferred to standard medium supplemented or not with 50 or 500 nM eBL for 5 days. In these tests, the root system was placed in the dark. For evaluation of the hypocotyl elongation in the light or in the dark, the *cml8* mutant lines and the reference line were sown on standard or supplemented medium containing eBL (250/500 nM to 1 μM). For the dark-grown seedlings, germination induction was triggered by 6 h of light in a culture chamber at 20/22°C and 40% humidity. The dishes were then placed in the dark and maintained under the same temperature and humidity conditions for 5 days. The light-grown seedlings were placed in a culture chamber at 20/22°C and 40% humidity with a 16-h photoperiod for 5 days. Images of the seedlings were acquired with an Epson Expression 12000XL high-resolution scanner (Epson, Suwa, Japan). The length of the PR, etiolated hypocotyls, and the light-grown hypocotyls were measured on the acquired images using the ImageJ software (Schindelin et al., 2015) and the NeuronJ plugin (Meijering et al., 2004).

Histochemical GUS activity analysis

A homozygous transgenic line expressing a construct with the CML8 promoter (1.5 kb) fused to the *uidA* (Zhu et al., 2017) gene was used. 7-day-old seedlings were treated or not with 1 μM eBL for 3 h. Histochemical staining for GUS activity was performed as described by Magnan *et al.* (Magnan et al., 2008). The resulting samples were observed under a stereomicroscope Axio Zoom.V16 (Zeiss, Oberkochen, Germany). The images illustrated are representative of at least three independent observations with similar expression patterns.

RNA isolation and RNA-seq analysis

The analyses were carried out using 10-day-old seedlings as biological. Plants of the different genotypes were grown at the same time on standard culture media and harvested at the same moment. The results presented are representative of the harvesting of three independent biological replicates. Total RNAs were extracted using E.Z.N.A® Plant RNA Kit (Omega Bio-tek, Norcross, GA, USA) according to the manufacturer protocol and treated with DNase (RNAse-free DNase I Set, Omega Bio-tek, Norcross, GA, USA). RNAseq was performed at the GeT-PlaGe core facility, INRAe Toulouse. RNA-seq libraries have been prepared according to Illumina's protocols using the Illumina TruSeq Stranded mRNA sample prep kit to analyze mRNA. Briefly, mRNAs were selected using poly-T beads. Then, RNAs were fragmented to generate double-stranded cDNA, and adaptators were ligated to be sequenced. 11 cycles of PCR were applied to amplify libraries. Library quality was assessed using a Fragment Analyzer, and libraries were quantified by qPCR using the Kapa Library Quantification Kit. RNA-seq experiments have been performed on an Illumina NovaSeq 6000 using a paired-end read length of 2 × 150 pb with the Illumina NovaSeq 6000 sequencing kits.

Statistical analysis of RNA-seq data

The analyses were performed as described in Zhu et al. (2021). RNAseq cleanup (fastq) was performed with TrimGalore-0.4.5 (option, Illumina). Pair-end reads from the 9 RNAseq runs were aligned on the Arabidopsis TAIR10 genome with an aligner that considers splicing sites, hisat2-2.1.0. The obtained alignments were sorted by name: samtools sort -n and the counting was done with HTSeq-0.9.1. An average of 36 million reads with quality scores over 90% per sample were obtained. To perform differential analysis, *htseq*-counts files were analyzed with the R software using the EdgeR package version 3.24.3 (McCarthy et al., 2012). A genotype comparison between WT and *cml8* genotypes was performed. Genes that failed to have at least 1 read after a count per million normalizations in at least one half of the samples were excluded. Next, the raw counts were normalized using TMM method, and count distribution was modeled with a negative binomial generalized linear model where the genotype and the

replicate were taken into accounts and the dispersion estimated by the EdgeR method. A likelihood ratio test was performed to assess a genotype effect. Raw *P*-values were corrected with the Benjamini-Hochberg procedure to adjust the false discovery rate (FDR). A gene was considered differentially expressed if its adjusted *P*-value was ≤0.05. A list of DEGs was recovered for both WT versus KO *cml8* and WT versus OE *CML8* comparisons based on a 5% FDR correction (Data S1).

RT-qPCR analyses

Gene expression analyses were carried out on a material from 7-day-old *Arabidopsis* seedlings and quantified under different conditions by RT-qPCR under standard culture conditions or in kinetic response to exogenous application of eBL (1 μM). To obtain spatial information on *CML8* expression profile, aerial parts (cotyledons and hypocotyl) were harvested separately from the root system. For each RT-qPCR experiment, total RNAs from at least three biological replicates were extracted as described in the section above "RNA isolation and RNA-seq analysis." The tested genes were as follows: *CML8* (AT4G14640), *BRI1* (AT4G39400), *BAK1* (AT4G33430), *DWF7* (AT3G02580), *DWF4* (AT3G50660), *CPD* (AT5G05690), *SAUR15* (AT4G38850), *BAS1* (AT2G26710), and *TIP41* (AT4G34270). The sequences of the primers used are referenced in Table S1. The qPCR on cDNA dilutions from at least three independent biological replicates were performed on CFX Opus 384 Real Time PCR system (Bio Rad, Hercules, CA, USA). Three technical replicates were performed for each analysis. The *TIP41* gene was used for data normalization (Czechowski et al., 2005), and data analysis was performed using the ΔΔCt method (Schmittgen & Livak, 2008).

Sub-cellular localization of BRI1 and CML8

The coding sequences of *CML8* have been cloned under the control of the constitutive Arabidopsis Ubiquitin10 promoter and tagged with a mCHERRY fluorescent protein. The *pAtUbi10*::BRI1::mCitrine construct was provided by G. Vert. *A. tumefaciens* transformed with the constructs were infiltrated into *N. benthamiana* leaves as described by Lindbo (2007) with minor modifications. Bacteria were suspended in infiltration buffer (10 mM MES/KOH pH 5.7, 10 mM $MgCl_2$, 150 μM Acetosyringone; Merck, Darmstadt, Germany) to achieve an OD_{600nm} = 0.3. Two days after infiltration, the localization of the proteins was examined by confocal microscopy. Imaging was performed on a Leica TCS SP8 laser scanning microscope (Leica Microsystems, Wetlzlar, Germany). The fluorescence of mCitrine and mCHERRY was excited using a 488 nm argon laser and a 561 nm diode laser, respectively. Fluorescence emission was captured at 500–550 nm and 580–650 nm, respectively. The images were processed using Leica Lite software (Leica Microsystems, Wetlzlar, Germany). The data shown in this article are representative of at least three independent biological replicates.

In planta protein–protein interaction by co-immunoprecipitation (Co-IP) experiments

The *p35S::CML8::6HA, p35S::AtCaM2::6HA, p35S::CML42::6HA, pAtUbi10*::BRI1::mCitrine, and *p35S::GFP* constructs were agroinfiltrated into *N. benthamiana* leaves as described in "Sub-cellular localization of BRI1 and CML8." For Co-IP analyses, leaf samples were collected at 48 h post-inoculation as described by Kadota et al. (2016). Experiments investigating the influence of ligand binding on BRI1–CML8 interaction involved treatment of inoculated leaves with either 1 μM eBL or water (mock) for 2 h prior to liquid nitrogen freezing. The total proteins of the leaves ("INPUT") were isolated after grinding the samples in liquid nitrogen to a fine powder which was collected (at 2 mL/g) in the extraction buffer and incubated 30 min at 4°C (Kadota et al., 2016). Samples were cleared from cell debris by centrifugation and filtration. For Co-IP assays, the m-Citrine or GFP-tagged proteins present in the solubilized fraction are then immunoprecipitated with their respective interactors using the μMACSTM GFP Isolation kit (Miltenyi Biotec, Bergisch Gladbach, Germany) according to the manufacturer protocol. For the GFP control, immunoprecipitation was performed directly from the extracted total proteins resuspended in the lysis buffer of the μMACS kit™ GFP Isolation supplemented with a protease inhibitor cocktail (Merck, Darmstadt, Germany). The following steps remain the same. Detection of the proteins of interest after Co-IP was performed by Western blot analysis. Proteins were loaded onto a 10% SDS-PAGE gel (TGX™ FastCast™ Acrylamide Kit, 10%; BioRad, Hercules, CA, USA) and transferred to a nitrocellulose membrane (Amersham™ Protran® Western blotting membranes, nitrocellulose; Merck, Darmstadt, Germany). Detection of BRI1::mCitrine and GFP was performed with an anti-GFP primary antibody (GFP Polyclonal Antibody; Thermo Fisher Scientific, Waltham, MA, USA), coupled to the horseradish peroxidase (HRP)-conjugated anti-rabbit secondary antibody (Rabbit TrueBlot®: Anti-Rabbit IgG HRP, Rockland, Philadelphia, PA, USA). Similarly, detection of CML8::6HA, CaM2::6HA, or CML42::6HA protein was performed using HRP-conjugated anti-HA antibody (Anti-HA-Peroxidase High Affinity, Roche, Basel, Switzerland). Protein revelation was performed with SuperSignal™ West Dura (Thermo Fisher Scientific, Waltham, MA, USA) and Western blot imaging on the ChemiDoc™ MP Imaging System (BioRad, Hercules, CA, USA).

BR signaling pathway activation state

The crushed 7-day-old seedlings were resuspended in 2X Laemmli, and BES1 protein detection was performed by Western blot analysis as described in "In planta protein–protein interaction by co-immunoprecipitation experiments" using a primary α-BES1 antibody (Yu et al., 2011) coupled to a secondary antibody conjugated to HRP (Goat anti-Rabbit IgG (H&L), HRP conjugated, Agrisera, Vännäs, Sweden). For each plant line, and each of the four biological replicates, the BES1/pBES1 ratio is established using Image Lab's "Volume Tools" quantification tool (Bio Rad, Hercules, CA, USA).

Statistical analyses

For each phenotypic analysis, at least three biological replicates were performed. For each replicate at least 30–40 values per genotype obtained. For the light grown hypocotyl experiment, the results presented correspond to a biological replicate composed of 40–50 values per genotype. For the RT-qPCR analyses, three biological replicates and three technical replicates were performed. For each analyzed gene, n = 8–9. Statistical analyses were performed using GraphPad Prism for Windows (GraphPad Software, San Diego, CA, USA). A two-way ANOVA was used to analyze data with multiple factors, while the Wilcoxon–Mann–Whitney test was used for non-parametric data sets with two groups. Asterisks indicate statistically significant differences. See the figure legends for details on specific *P* values.

ACCESSION NUMBERS

CML8 (AT4G14640), CaM2 (AT2G41110), CML42 (AT4G20780), *BRI1* (AT4G39400), *BES1* (AT1G19350), *BZR1* (AT1G75080), *BAK1* (AT4G33430), *DWF7* (AT3G02580), *DWF4*

(AT3G50660), *CPD* (AT5G05690), *SAUR15* (AT4G38850), *BAS1* (AT2G26710), *TIP41* (AT4G34270).

AUTHOR CONTRIBUTIONS

AL, J-PG, and DA conceived and designed the project. AL and ER performed molecular cloning, RNA extraction, cDNA synthesis, and RT-qPCR analysis; AL and HF performed the Co-IP experiments; all experiments were independently reproduced in the laboratory. MA, HSC, AL, and DA carried out RNA-seq analyses. AL and DA analyzed and interpreted the data and wrote the manuscript. GV, MM, and J-PG critically revised the manuscript. All authors have read and agreed to the published version of the manuscript.

ACKNOWLEDGMENTS

A.L. is the recipient of a fellowship from the French Ministry of National Education and Research. We are grateful to Sophie Valière and Tabatha Bulach at the GeT-PlaGe platform for RNA-seq libraries and sequencing. We would like to thank Artemis Perraki for her careful review of the manuscript and her insightful suggestions. This work was supported by the Université Paul Sabatier (Toulouse, France), the CNRS (France), and by the Agence Nationale de la Recherche (ANR) (ANR-17-CE20-0017-01) thanks to the CaPPTure project. This study is set within the framework of the "Laboratoires d'Excellences (LABEX)" TULIP (ANR-10-LABX-41) and of the "École Universitaire de Recherche (EUR)" TULIP-GS (ANR-18-EURE-0019).

CONFLICT OF INTEREST

All the authors have approved the submitted version of the manuscript and declare no conflicts of interest.

DATA AVAILABILITY STATEMENT

Correspondence and requests for materials should be addressed to didier.aldon@univ-tlse3.fr. All relevant data can be found within the manuscript and its supporting materials.

SUPPORTING INFORMATION

Additional Supporting Information may be found in the online version of this article.

Data S1. List of all genes differentially regulated between KO *cml8* and WT (Col).

Data S2. List of all genes differentially regulated (up- or down-) between OE *CML8* and WT (Col).

Data S3. List of all genes identified as BR responsive among the DEGs identified in cml8 genotypes.

Figure S1. The *CML8* gene is expressed mainly in root tissues in young *A. thaliana* seedlings.

Figure S2. Molecular characterization of the *cml8.2* mutant T-DNA line (SALK_022524C) and the corresponding complemented line (*cml8.2_C#13*) in the Columbia-8 accession.

Figure S3. Root growth responses of WT, *CML8* overexpression line 2 (*OE CML8 3.2*), and the complemented line (*cml8.2_C#13*) were investigated under standard conditions and following epibrassinolide (eBL) treatment.

Figure S4. Analysis of the effect of light/darkness on hypocotyl elongation in WT and *CML8* overexpression line 2 (OE2) seedlings under standard conditions or following eBL treatment.

Figure S5. Analysis of the effect of light/darkness on hypocotyl elongation in WT and complemented line *cml8.2_C#13* seedlings under standard conditions or treated with eBL.

Figure S6. Comparative expression profile analysis of *CML8* (AT4g14640) and *BRI1* (AT4G39400) using the CoNekT expression profile comparison tool (https://conekt.sbs.ntu.edu.sg).

Figure S7. Assessing the specificity of CML8–BRI1 interaction with co-IP controls.

Figure S8. Expression analysis of brassinosteroid homeostasis and signaling marker genes in *cml8* mutants following eBL treatment.

Table S1. Primers for quantitative RT-PCR (RT-qPCR) and characterization of the KO *cml8* mutant.

REFERENCES

Ackerman-Lavert, M. & **Savaldi-Goldstein, S.** (2020) Growth models from a brassinosteroid perspective. *Current Opinion in Plant Biology*, **53**, 90–97.

Aldon, D., **Mbengue, M.**, **Mazars, C.** & **Galaud, J.P.** (2018) Calcium Signalling in plant biotic interactions. *International Journal of Molecular Sciences*, **19**, 665.

Bender, K.W., **Rosenbaum, D.M.**, **Vanderbeld, B.**, **Ubaid, M.** & **Snedden, W.A.** (2013) The Arabidopsis calmodulin-like protein, CML39, functions during early seedling establishment. *The Plant Journal*, **76**, 634–647.

Benkova, E. (2016) Plant hormones in interactions with the environment. *Plant Molecular Biology*, **91**, 597.

Bouche, N., **Yellin, A.**, **Snedden, W.A.** & **Fromm, H.** (2005) Plant-specific calmodulin-binding proteins. *Annual Review of Plant Biology*, **56**, 435–466.

Chaiwanon, J. & **Wang, Z.Y.** (2015) Spatiotemporal brassinosteroid signaling and antagonism with auxin pattern stem cell dynamics in Arabidopsis roots. *Current Biology*, **25**, 1031–1042.

Chaiwanon, J., **Wang, W.**, **Zhu, J.Y.**, **Oh, E.** & **Wang, Z.Y.** (2016) Information integration and communication in plant growth regulation. *Cell*, **164**, 1257–1268.

Challa, K.R., **Aggarwal, P.** & **Nath, U.** (2016) Activation of YUCCA5 by the transcription factor TCP4 integrates developmental and environmental signals to promote hypocotyl elongation in Arabidopsis. *Plant Cell*, **28**, 2117–2130.

Chin, D. & **Means, A.R.** (2000) Calmodulin: a prototypical calcium sensor. *Trends in Cell Biology*, **10**, 322–328.

Choi, S., **Cho, Y.H.**, **Kim, K.**, **Matsui, M.**, **Son, S.H.**, **Kim, S.K.** ***et al.*** (2013) BAT1, a putative acyltransferase, modulates brassinosteroid levels in Arabidopsis. *The Plant Journal*, **73**, 380–391.

Chung, Y., **Maharjan, P.M.**, **Lee, O.**, **Fujioka, S.**, **Jang, S.**, **Kim, B.** ***et al.*** (2011) Auxin stimulates DWARF4 expression and brassinosteroid biosynthesis in Arabidopsis. *The Plant Journal*, **66**, 564–578.

Clark, N.M., **Nolan, T.M.**, **Wang, P.**, **Song, G.**, **Montes, C.**, **Valentine, C.T.** ***et al.*** (2021) Integrated omics networks reveal the temporal signaling events of brassinosteroid response in Arabidopsis. *Nature Communications*, **12**, 5858.

Clouse, S.D. & **Sasse, J.M.** (1998) BRASSINOSTEROIDS: essential regulators of plant growth and development. *Annual Review of Plant Physiology and Plant Molecular Biology*, **49**, 427–451.

Clouse, S.D., **Langford, M.** & **McMorris, T.C.** (1996) A brassinosteroid-insensitive mutant in Arabidopsis thaliana exhibits multiple defects in growth and development. *Plant Physiology*, **111**, 671–678.

Czechowski, T., **Stitt, M.**, **Altmann, T.**, **Udvardi, M.K.** & **Scheible, W.R.** (2005) Genome-wide identification and testing of superior reference genes for transcript normalization in Arabidopsis. *Plant Physiology*, **139**, 5–17.

Davis, T.N., **Urdea, M.S.**, **Masiarz, F.R.** & **Thorner, J.** (1986) Isolation of the yeast calmodulin gene: calmodulin is an essential protein. *Cell*, **47**, 423–431.

Delesalle, C., **Vert, G.** & **Fujita, S.** (2024) The cell surface is the place to be for brassinosteroid perception and responses. *Nature Plants*, **10**, 206–218.

Du, L. & **Poovaiah, B.W.** (2005) Ca2+/calmodulin is critical for brassinosteroid biosynthesis and plant growth. *Nature*, **437**, 741–745.

Dubrovsky, J.G. & **Forde, B.G.** (2012) Quantitative analysis of lateral root development: pitfalls and how to avoid them. *Plant Cell*, **24**, 4–14.

Edel, K.H., **Marchadier, E.**, **Brownlee, C.**, **Kudla, J.** & **Hetherington, A.M.** (2017) The evolution of calcium-based Signalling in plants. *Current Biology*, **27**, R667–R679.

Goda, H., **Sawa, S.**, **Asami, T.**, **Fujioka, S.**, **Shimada, Y.** & **Yoshida, S.** (2004) Comprehensive comparison of auxin-regulated and brassinosteroid-regulated genes in Arabidopsis. *Plant Physiology*, **134**, 1555–1573.

Gonzalez-Garcia, M.P., **Vilarrasa-Blasi, J.**, **Zhiponova, M.**, **Divol, F.**, **Mora-Garcia, S.**, **Russinova, E.** ***et al.*** (2011) Brassinosteroids control meristem size by promoting cell cycle progression in Arabidopsis roots. *Development*, **138**, 849–859.

Halter, T., **Imkampe, J.**, **Mazzotta, S.**, **Wierzba, M.**, **Postel, S.**, **Bucherl, C.** ***et al.*** (2014) The leucine-rich repeat receptor kinase BIR2 is a negative regulator of BAK1 in plant immunity. *Current Biology*, **24**, 134–143.

He, Z., **Wang, Z.Y.**, **Li, J.**, **Zhu, Q.**, **Lamb, C.**, **Ronald, P.** ***et al.*** (2000) Perception of brassinosteroids by the extracellular domain of the receptor kinase BRI1. *Science*, **288**, 2360–2363.

Hepler, P.K. (2005) Calcium: a central regulator of plant growth and development. *Plant Cell*, **17**, 2142–2155.

Hruz, T., **Laule, O.**, **Szabo, G.**, **Wessendorp, F.**, **Bleuler, S.**, **Oertle, L.** ***et al.*** (2008) Genevestigator v3: a reference expression database for the meta-analysis of transcriptomes. *Advances in Bioinformatics*, **2008**, 420747.

Huang da, W., **Sherman, B.T.** & **Lempicki, R.A.** (2009) Systematic and integrative analysis of large gene lists using DAVID bioinformatics resources. *Nature Protocols*, **4**, 44–57.

Ibanes, M., **Fabregas, N.**, **Chory, J.** & **Cano-Delgado, A.I.** (2009) Brassinosteroid signaling and auxin transport are required to establish the periodic pattern of Arabidopsis shoot vascular bundles. *Proceedings of the National Academy of Sciences of the United States of America*, **106**, 13630–13635.

Iqbal, Z., **Shariq Iqbal, M.**, **Singh, S.P.** & **Buaboocha, T.** (2020) Ca(2+)/Calmodulin complex triggers CAMTA transcriptional machinery under stress in plants: signaling Cascade and molecular regulation. *Frontiers in Plant Science*, **11**, 598327.

Kadota, Y., **Macho, A.P.** & **Zipfel, C.** (2016) Immunoprecipitation of plasma membrane receptor-like kinases for identification of phosphorylation sites and associated proteins. *Methods in Molecular Biology*, **1363**, 133–144.

Kim, B., **Jeong, Y.J.**, **Corvalan, C.**, **Fujioka, S.**, **Cho, S.**, **Park, T.** ***et al.*** (2014) Darkness and gulliver2/phyB mutation decrease the abundance of phosphorylated BZR1 to activate brassinosteroid signaling in Arabidopsis. *The Plant Journal*, **77**, 737–747.

Kim, S.H., **Lee, S.H.**, **Park, T.K.**, **Tian, Y.**, **Yu, K.**, **Lee, B.H.** ***et al.*** (2024) Comparative analysis of BZR1/BES1 family transcription factors in Arabidopsis. *The Plant Journal*, **117**, 747–765.

Kim, T.W. & **Wang, Z.Y.** (2010) Brassinosteroid signal transduction from receptor kinases to transcription factors. *Annual Review of Plant Biology*, **61**, 681–704.

Leba, L.J., **Cheval, C.**, **Ortiz-Martin, I.**, **Ranty, B.**, **Beuzon, C.R.**, **Galaud, J.P.** ***et al.*** (2012) CML9, an Arabidopsis calmodulin-like protein, contributes to plant innate immunity through a flagellin-dependent signalling pathway. *The Plant Journal*, **71**, 976–989.

Leitao, N., **Dangeville, P.**, **Carter, R.** & **Charpentier, M.** (2019) Nuclear calcium signatures are associated with root development. *Nature Communications*, **10**, 4865.

Li, C., **Zhang, S.** & **Wang, X.** (2017) Novel signaling Interface constituted with membrane receptor-like kinases emerged from the study of interaction and Transphosphorylation of BRI1 and BAK1. *Current Topics in Medicinal Chemistry*, **17**, 2393–2400.

Li, Q.F., **Lu, J.**, **Yu, J.W.**, **Zhang, C.Q.**, **He, J.X.** & **Liu, Q.Q.** (2018) The brassinosteroid-regulated transcription factors BZR1/BES1 function as a coordinator in multisignal-regulated plant growth. *Biochimica et Biophysica Acta, Gene Regulatory Mechanisms*, **1861**, 561–571.

Lin, F., **Cao, J.**, **Yuan, J.**, **Liang, Y.** & **Li, J.** (2021) Integration of light and Brassinosteroid signaling during seedling establishment. *International Journal of Molecular Sciences*, **22**, 12971.

Lindbo, J.A. (2007) High-efficiency protein expression in plants from agroinfection-compatible tobacco mosaic virus expression vectors. *BMC Biotechnology*, **7**, 52.

Luan, S. & **Wang, C.** (2021) Calcium signaling mechanisms across kingdoms. *Annual Review of Cell and Developmental Biology*, **37**, 311–340.

Magnan, F., **Ranty, B.**, **Charpenteau, M.**, **Sotta, B.**, **Galaud, J.P.** & **Aldon, D.** (2008) Mutations in AtCML9, a calmodulin-like protein from Arabidopsis thaliana, alter plant responses to abiotic stress and abscisic acid. *The Plant Journal*, **56**, 575–589.

Marsolais, F., **Boyd, J.**, **Paredes, Y.**, **Schinas, A.M.**, **Garcia, M.**, **Elzein, S.** ***et al.*** (2007) Molecular and biochemical characterization of two brassinosteroid sulfotransferases from Arabidopsis, AtST4a (At2g14920) and AtST1 (At2g03760). *Planta*, **225**, 1233–1244.

McAinsh, M.R. & **Pittman, J.K.** (2009) Shaping the calcium signature. *The New Phytologist*, **181**, 275–294.

McCarthy, D.J., **Chen, Y.** & **Smyth, G.K.** (2012) Differential expression analysis of multifactor RNA-Seq experiments with respect to biological variation. *Nucleic Acids Research*, **40**, 4288–4297.

McCormack, E. & **Braam, J.** (2003) Calmodulins and related potential calcium sensors of Arabidopsis. *The New Phytologist*, **159**, 585–598.

McCormack, E., **Tsai, Y.C.** & **Braam, J.** (2005) Handling calcium signaling: Arabidopsis CaMs and CMLs. *Trends in Plant Science*, **10**, 383–389.

Meijering, E., **Jacob, M.**, **Sarria, J.C.**, **Steiner, P.**, **Hirling, H.** & **Unser, M.** (2004) Design and validation of a tool for neurite tracing and analysis in fluorescence microscopy images. *Cytometry. Part A*, **58**, 167–176.

Mussig, C., **Shin, G.H.** & **Altmann, T.** (2003) Brassinosteroids promote root growth in Arabidopsis. *Plant Physiology*, **133**, 1261–1271.

Nakamoto, D., **Ikeura, A.**, **Asami, T.** & **Yamamoto, K.T.** (2006) Inhibition of brassinosteroid biosynthesis by either a dwarf4 mutation or a brassinosteroid biosynthesis inhibitor rescues defects in tropic responses of hypocotyls in the arabidopsis mutant nonphototropic hypocotyl 4. *Plant Physiology*, **141**, 456–464.

Neff, M.M., **Nguyen, S.M.**, **Malancharuvil, E.J.**, **Fujioka, S.**, **Noguchi, T.**, **Seto, H.** ***et al.*** (1999) BAS1: a gene regulating brassinosteroid levels and light responsiveness in Arabidopsis. *Proceedings of the National Academy of Sciences of the United States of America*, **96**, 15316–15323.

Nemhauser, J.L., **Mockler, T.C.** & **Chory, J.** (2004) Interdependency of brassinosteroid and auxin signaling in Arabidopsis. *PLoS Biology*, **2**, E258.

Nolan, T., **Liu, S.**, **Guo, H.**, **Li, L.**, **Schnable, P.** & **Yin, Y.** (2017) Identification of Brassinosteroid Target Genes by Chromatin Immunoprecipitation Followed by High-Throughput Sequencing (ChIP-seq) and RNA-Sequencing. *Methods in Molecular Biology*, **1564**, 63–79.

Nolan, T.M., **Vukasinovic, N.**, **Hsu, C.W.**, **Zhang, J.**, **Vanhoutte, I.**, **Shahan, R.** ***et al.*** (2023) Brassinosteroid gene regulatory networks at cellular resolution in the Arabidopsis root. *Science*, **379**, eadf4721.

Obayashi, T., **Hibara, H.**, **Kagaya, Y.**, **Aoki, Y.** & **Kinoshita, K.** (2022) ATTED-II v11: a plant gene Coexpression database using a sample balancing technique by Subagging of principal components. *Plant & Cell Physiology*, **63**, 869–881.

Oh, E., **Zhu, J.Y.**, **Bai, M.Y.**, **Arenhart, R.A.**, **Sun, Y.** & **Wang, Z.Y.** (2014) Cell elongation is regulated through a central circuit of interacting transcription factors in the Arabidopsis hypocotyl. *eLife*, **3**, e03031.

Oh, M.H., **Kim, H.S.**, **Wu, X.**, **Clouse, S.D.**, **Zielinski, R.E.** & **Huber, S.C.** (2012) Calcium/calmodulin inhibition of the Arabidopsis BRASSINOSTEROID-INSENSITIVE 1 receptor kinase provides a possible link between calcium and brassinosteroid signalling. *The Biochemical Journal*, **443**, 515–523.

Perochon, A., **Aldon, D.**, **Galaud, J.P.** & **Ranty, B.** (2011) Calmodulin and calmodulin-like proteins in plant calcium signaling. *Biochimie*, **93**, 2048–2053.

Ranty, B., **Aldon, D.**, **Cotelle, V.**, **Galaud, J.P.**, **Thuleau, P.** & **Mazars, C.** (2016) Calcium sensors as key hubs in plant responses to biotic and abiotic stresses. *Frontiers in Plant Science*, **7**, 327.

Ren, H. & **Gray, W.M.** (2015) SAUR proteins as effectors of hormonal and environmental signals in plant growth. *Molecular Plant*, **8**, 1153–1164.

Schindelin, J., **Rueden, C.T.**, **Hiner, M.C.** & **Eliceiri, K.W.** (2015) The ImageJ ecosystem: an open platform for biomedical image analysis. *Molecular Reproduction and Development*, **82**, 518–529.

Schmittgen, T.D. & **Livak, K.J.** (2008) Analyzing real-time PCR data by the comparative C(T) method. *Nature Protocols*, **3**, 1101–1108.

Scholz, S.S., **Vadassery, J.**, **Heyer, M.**, **Reichelt, M.**, **Bender, K.W.**, **Snedden, W.A.** ***et al.*** (2014) Mutation of the Arabidopsis calmodulin-like protein CML37 deregulates the jasmonate pathway and enhances susceptibility to herbivory. *Molecular Plant*, **7**, 1712–1726.

Shahan, R., **Hsu, C.W.**, **Nolan, T.M.**, **Cole, B.J.**, **Taylor, I.W.**, **Greenstreet, L.** ***et al.*** (2022) A single-cell Arabidopsis root atlas reveals developmental trajectories in wild-type and cell identity mutants. *Developmental Cell*, **57**, 543–560.e9.

Sherman, B.T., **Hao, M.**, **Qiu, J.**, **Jiao, X.**, **Baseler, M.W.**, **Lane, H.C.** ***et al.*** (2022) DAVID: a web server for functional enrichment analysis and functional annotation of gene lists (2021 update). *Nucleic Acids Research*, **50**, W216–W221.

Snedden, W.A. & **Fromm, H.** (2001) Calmodulin as a versatile calcium signal transducer in plants. *New Phytologist*, **151**, 35–66.

Song, X., **Li, J.**, **Lyu, M.**, **Kong, X.**, **Hu, S.**, **Song, Q.** ***et al.*** (2021) CALMODULIN-LIKE-38 and PEP1 RECEPTOR 2 integrate nitrate and brassinosteroid signals to regulate root growth. *Plant Physiology*, **187**, 1779–1794.

Sun, Q., **Huang, R.**, **Zhu, H.**, **Sun, Y.** & **Guo, Z.** (2021) A novel Medicago truncatula calmodulin-like protein (MtCML42) regulates cold tolerance and flowering time. *The Plant Journal*, **108**, 1069–1082.

Sun, Y., **Fan, X.Y.**, **Cao, D.M.**, **Tang, W.**, **He, K.**, **Zhu, J.Y.** ***et al.*** (2010) Integration of brassinosteroid signal transduction with the transcription network for plant growth regulation in Arabidopsis. *Developmental Cell*, **19**, 765–777.

Symonds, K., **Teresinski, H.**, **Hau, B.**, **Chiasson, D.**, **Benidickson, K.**, **Plaxton, W.** ***et al.*** (2024) Arabidopsis CML13 and CML14 have essential and overlapping roles in plant development. *Plant & Cell Physiology*, **65**, 228–242.

Symonds, K., **Teresinski, H.J.**, **Hau, B.**, **Dwivedi, V.**, **Belausov, E.**, **Bar-Sinai, S.** ***et al.*** (2024) Functional characterization of Calmodulin-like proteins, CML13 and CML14, as novel light chains of Arabidopsis class VIII Myosins. *Journal of Experimental Botany*, **75**, 2313–2329.

Tanaka, K., **Asami, T.**, **Yoshida, S.**, **Nakamura, Y.**, **Matsuo, T.** & **Okamoto, S.** (2005) Brassinosteroid homeostasis in Arabidopsis is ensured by feedback expressions of multiple genes involved in its metabolism. *Plant Physiology*, **138**, 1117–1125.

Tanaka, K., **Nakamura, Y.**, **Asami, T.**, **Yoshida, S.**, **Matsuo, T.** & **Okamoto, S.** (2003) Physiological roles of brassinosteroids in early growth of Arabidopsis: brassinosteroids have a synergistic relationship with gibberellin as well as auxin in light-grown hypocotyl elongation. *Journal of Plant Growth Regulation*, **22**, 259–271.

Tian, H., **Lv, B.**, **Ding, T.**, **Bai, M.** & **Ding, Z.** (2017) Auxin-BR interaction regulates plant growth and development. *Frontiers in Plant Science*, **8**, 2256.

Tian, W., **Wang, C.**, **Gao, Q.**, **Li, L.** & **Luan, S.** (2020) Calcium spikes, waves and oscillations in plant development and biotic interactions. *Nature Plants*, **6**, 750–759.

Turk, E.M., **Fujioka, S.**, **Seto, H.**, **Shimada, Y.**, **Takatsuto, S.**, **Yoshida, S.** ***et al.*** (2003) CYP72B1 inactivates brassinosteroid hormones: an intersection between photomorphogenesis and plant steroid signal transduction. *Plant Physiology*, **133**, 1643–1653.

Vadassery, J., **Reichelt, M.**, **Hause, B.**, **Gershenzon, J.**, **Boland, W.** & **Mithofer, A.** (2012) CML42-mediated calcium signaling coordinates responses to Spodoptera herbivory and abiotic stresses in Arabidopsis. *Plant Physiology*, **159**, 1159–1175.

Vanstraelen, M. & **Benkova, E.** (2012) Hormonal interactions in the regulation of plant development. *Annual Review of Cell and Developmental Biology*, **28**, 463–487.

Villalobo, A. (2023) Regulation of ErbB receptors by the Ca(2+) sensor protein Calmodulin in cancer. *Biomedicine*, **11**, 661.

Vukasinovic, N., **Wang, Y.**, **Vanhoutte, I.**, **Fendrych, M.**, **Guo, B.**, **Kvasnica, M.** ***et al.*** (2021) Local brassinosteroid biosynthesis enables optimal root growth. *Nature Plants*, **7**, 619–632.

Wang, W., **Chen, Q.**, **Botella, J.R.** & **Guo, S.** (2019) Beyond light: insights into the role of constitutively Photomorphogenic1 in plant hormonal signaling. *Frontiers in Plant Science*, **10**, 557.

Wang, Z.Y., **Nakano, T.**, **Gendron, J.**, **He, J.**, **Chen, M.**, **Vafeados, D.** ***et al.*** (2002) Nuclear-localized BZR1 mediates brassinosteroid-induced growth and feedback suppression of brassinosteroid biosynthesis. *Developmental Cell*, **2**, 505–513.

Wei, Z. & **Li, J.** (2016) Brassinosteroids regulate root growth, development, and Symbiosis. *Molecular Plant*, **9**, 86–100.

Yin, Y., **Vafeados, D.**, **Tao, Y.**, **Yoshida, S.**, **Asami, T.** & **Chory, J.** (2005) A new class of transcription factors mediates brassinosteroid-regulated gene expression in Arabidopsis. *Cell*, **120**, 249–259.

Yin, Y., **Wang, Z.Y.**, **Mora-Garcia, S.**, **Li, J.**, **Yoshida, S.**, **Asami, T.** ***et al.*** (2002) BES1 accumulates in the nucleus in response to brassinosteroids to regulate gene expression and promote stem elongation. *Cell*, **109**, 181–191.

Yu, X., **Li, L.**, **Zola, J.**, **Aluru, M.**, **Ye, H.**, **Foudree, A.** ***et al.*** (2011) A brassinosteroid transcriptional network revealed by genome-wide identification of BESI target genes in Arabidopsis thaliana. *The Plant Journal*, **65**, 634–646.

Yu, Y., **Zhang, H.**, **Long, Y.**, **Shu, Y.** & **Zhai, J.** (2022) Plant public RNA-seq database: a comprehensive online database for expression analysis of ~45 000 plant public RNA-Seq libraries. *Plant Biotechnology Journal*, **20**, 806–808.

Zhang, H., **Zhang, F.**, **Yu, Y.**, **Feng, L.**, **Jia, J.**, **Liu, B.** ***et al.*** (2020) A comprehensive online database for exploring approximately 20,000 public Arabidopsis RNA-Seq libraries. *Molecular Plant*, **13**, 1231–1233.

Zhang, Y., **Liu, Z.**, **Wang, J.**, **Chen, Y.**, **Bi, Y.** & **He, J.** (2015) Brassinosteroid is required for sugar promotion of hypocotyl elongation in Arabidopsis in darkness. *Planta*, **242**, 881–893.

Zhao, Y., **Qi, Z.** & **Berkowitz, G.A.** (2013) Teaching an old hormone new tricks: cytosolic Ca2+ elevation involvement in plant brassinosteroid signal transduction cascades. *Plant Physiology*, **163**, 555–565.

Zhu, J.Y., **Sae-Seaw, J.** & **Wang, Z.Y.** (2013) Brassinosteroid signalling. *Development*, **140**, 1615–1620.

Zhu, X., **Dunand, C.**, **Snedden, W.** & **Galaud, J.P.** (2015) CaM and CML emergence in the green lineage. *Trends in Plant Science*, **20**, 483–489.

Zhu, X., **Mazard, J.**, **Robe, E.**, **Pignoly, S.**, **Aguilar, M.**, **San Clemente, H.** ***et al.*** (2021) The same against many: AtCML8, a Ca(2+) sensor acting as a positive regulator of defense responses against several plant pathogens. *International Journal of Molecular Sciences*, **22**, 10469.

Zhu, X., **Robe, E.**, **Jomat, L.**, **Aldon, D.**, **Mazars, C.** & **Galaud, J.P.** (2017) CML8, an Arabidopsis Calmodulin-like protein, plays a role in pseudomonas syringae plant immunity. *Plant & Cell Physiology*, **58**, 307–319.

Zielinski, R.E. (2002) Characterization of three new members of the Arabidopsis thaliana calmodulin gene family: conserved and highly diverged members of the gene family functionally complement a yeast calmodulin null. *Planta*, **214**, 446–455.

Zogopoulos, V.L., **Saxami, G.**, **Malatras, A.**, **Angelopoulou, A.**, **Jen, C.H.**, **Duddy, W.J.** ***et al.*** (2021) Arabidopsis Coexpression tool: a tool for gene coexpression analysis in Arabidopsis thaliana. *iScience*, **24**, 102848.